2017

Fluorescent Probe Development for Fructose Specific Transporters in Cancer

Joseph Fedie
Michigan Technological University, jrfedie@mtu.edu

FLUORESCENT PROBE DEVELOPMENT FOR FRUCTOSE SPECIFIC TRANSPORTERS IN CANCER

By

Joseph R. Fedie

A THESIS

Submitted in partial fulfillment of the requirements for the degree of

MASTER OF SCIENCE

In Chemistry

MICHIGAN TECHNOLOGICAL UNIVERSITY

2017

This thesis has been approved in partial fulfillment of the requirements for the Degree of MASTER OF SCIENCE in Chemistry.

Department of Chemistry

Thesis Advisor: *Dr. Marina Tanasova*

Committee Member: *Dr. Tarun Dam*

Committee Member: *Dr. Shiyue Fang*

Department Chair: *Dr. Cary Chabalowski*

Table of Contents

List of Figures and Schemes

Preface

All contents of Chapter 1, 3 and 4 were written by Mr. Joseph R. Fedie and revised by Dr. Marina Tanasova. The contained material in Chapter 2 is currently in preparation for submission to a journal.

All of research done in Chapter 3 was conducted by Joseph R. Fedie with exceptions of (i) ManCou synthesis and purification which was performed by Mr. Shuai Xia; (ii) multicellular line comparison studies which were performed by Mr. Srinivas Kannan and Dr. Smitha Malalur Nagaraja Rao.

Acknowledgements

The amount of people to thank in helping me reach this point is innumerable and to properly thank each of them is fairly impossible but I am going to try. First of all I would like to thank my advisor and mentor Dr. Marina Tanasova for taking a chance on a rural farm boy from the middle of nowhere. Her continued support, trust and encouragement throughout the past three years. I have never met anyone with as much passion and love for science and her willingness to pass down that knowledge and training to me is something I never dreamed of. The skills and knowledge I have learned from her are boundless both as a scientist and as a person, I cannot overstate my appreciation and gratitude for her mentorship.

I would like to thank the members of my committee: Dr. Shiyue Fang and Tarun Dam both of whom have taught me much over the years at Michigan Tech both as a graduate and undergraduate student.

I would like to thank the current and former lab members: Andrew Perla, Erin Matthews, Dr. Lukasz Weselinski, Vagarshak Begoyan, Shuai Xia, and Morgan Charbonneau. All of whom I am very appreciated of their help over my time there and wish them all the best in their future careers.

I am incredibly grateful for all the help from the staff in the Department of Chemistry including Celine Grace, Denise Laux, Charlene Page, Kimberly McMullan, Dean Seppala, Don Wareham, Jerry Lutz, Joel Smith and Lois Blau. They all allowed me to focus more on my teaching and research without having to worry about orders or forms. I wish them all well in the future.

I am tremendously grateful to Lorri Reilly and Aparna Pandey whom both gave me the opportunity to learn and grow as an instructor and leader in the teaching labs. The knowledge and support from both of them is extraordinary and I wish them all the best.

I would like to thank my collaborators Srinivas Kannan and Dr. Smitha Rao for allowing use to their instruments and methods as well as sharing their advanced knowledge with me.

As for interdepartmental help I would like to thank Rashmi Adhikari for teaching me several biochemical techniques and overall patience. I would also like to thank Shahien Shahsavari and Ashok Khanal for their willingness to lend reagents and expertise.

I would like to thank Dr. Patricia Heiden for first introducing me into the realm of research as an undergrad and instilling the first spark of professional curiosity into me. For that I will always be grateful.

Thank you to my Michigan Tech colleges: Chelsea Nikula, Dr. Sasha Teymorian, Dr. Melanie Talaga, Dr. Ni Fan, Christian Welch and Soha Albukhari. They helped make graduate school more than just another job and I will always be thankful for that.

Finally, I would like to thank my parents and grandparents for the years of unconditional support from them. None of this would be possible without them, I will always love them and this dissertation is partially devoted to them.

List of Abbreviations

Å	Angstrom
Ac	Acetyl
Arg	Arginine
Asn	Asparagine
Asp	Aspartic Acid
Bn	Benzyl
C	Carboxy helix domain
DMSO	Dimethylsulfoxide
EDT	4,6-*O*-ethylidene-alpha-D-glucose
ESI	Electrospray Ionization
g	Gram
Gln	Glutamine
Glu	Glutamic Acid
Gly	Glycine
HPLC	High Performance Liquid Chromatography
ICH	Intercellular Helix
Ile	Isoleucine
MCF-7	Michigan Cancer Foundation-7
MFS	Major Facilitator Superfamily
mg	Milligram

mL	Milliliter
mM	Millimolar
MNBD	Mannitol Nitrobenzofurazan
N	Amino helix domain
NBD	Nitrobenzofurazan
NHI	N-hydroxy indole
NMR	Nuclear Magnetic Resonance
Pd	Palladium
PET	Positron Emission Topography
Phe	Phenylalanine
Pt	Platinum
SAR	Structural Activity Relationship
TLC	Thin Layer Chromotography
TM	Transmembrane Helix
Trp	Tryptophan
Tyr	Tyrosine
uL	Microliter
uM	Micromolar
UV-Vis	Ultraviolet-visible spectroscopay
Val	Valine

Abstract

Carbohydrate transporters or GLUTs of the major facilitator superfamily (MFS) are responsible for transporting sugars into the cell and have been of research interest for decades. Disruptions, mutations, and over-activations of GLUTs have been linked to a number of major diseases including cancer, obesity, and diabetes. Differentiating between transporters is incredibly difficult due to highly conserved structures, and so specific targeting between transporters has proven a complex challenge. GLUTs are highly flexible in their conformations however exactly what will and will not pass through the transporter is ambiguous at best, and many attempt to target these transporters have failed.

In an attempt to further understand GLUT5's transport capacity and specificity several probes were created by conjugating 1-amino-2,5-anhydro-D-mannitol with a number of fluorescent coumarins. These probes were then tested in cancer and normal breast cell lines to determine uptake mechanisms and transport specificity. To determine transport specificity probes were tested in the presence of competitive and non-competitive inhibitors. Probe analysis was carried out by evaluating the gained fluorescence of treated cells in a microplate setting and through confocal microscopy. Confocal imaging and Z-stack was utilized to understand the ability of the probe to pass into the cytosol or to remain in the cellular membrane. As a result, probes reflecting uptake capacity vs. membrane expression of the transporter were developed. The cumulative analysis of structure-uptake relationship for the developed probes gives insight into the capability of GLUT5 cargo transport and as well as a method for imaging GLUT5 in the cellular membrane.

Chapter 1

Introduction

1.1 GLUTs: classification and expression

GLUTs (facilitative glucose transporters) are expressed throughout the body and are vital for survival of cells. Gluts mediate a gradient dependent transport of carbohydrates into and out of the cell but cannot export their substrate's phosphorylated counterparts [1, 2]. There are fourteen known GLUTs and based on sequence, structural and substrate similarities are split into three major classes: Class I, II and III. Class I GLUTs (1-4 and 14) primarily facilitate uptake of glucose, but some are responsible for various other hexoses (Table 1). Class II GLUTs (5, 7, 9 and 11) are primarily fructose transporters, and Class III GLUTs (6, 8, 10, 12, and 13 (HMIT1)) are structurally atypical members of the GLUT family.

GLUT2-4 are relatively localized in specific areas. GLUT2 is mainly located in the liver and gastrointestinal tract. GLUT3 is primarily located in neuron cells and mainly transports glucose. GLUT4 is the unique of the class I transporters as it mainly reside inside the cell and is only brought to the surface in the presence of insulin. In low insulin concentrations, it resides in intracellular vesicles inside the cell membrane and is predominately present in skeletal and cardiac muscles [25]. GLUT4 has been found to have links with insulin resistance and diabetes and has been a potential therapeutic target [26].

Table 1. Glut Transporters

Class	Transporter	Expression in Normal Cells	Substrate
Class I	Glut1	erythrocytes	glucose, galactose
	Glut2	renal tubular, intestinal epithelial, liver and pancreatic β cells	glucose, galactose, fructose, glucosamine
	Glut3	neurons and placenta	glucose, galactose, mannose
	Glut4	adipose tissue and striated muscle	glucose, galactose, mannose, xylose
	Glut14	testis	glucose, galactose
Class II	Glut5	intestinal epithelial, erythrocytes, sperm	fructose
	Glut7	apical membrane in small and large intestine	glucose, fructose
	Glut9	liver, kidney and intestine	glucose, fructose
	Glut11	muscle, heart, fat, placenta, kidney, and pancreas	glucose, fructose
Class III	Glut 6	renal tubular, intestinal epithelial, liver and pancreatic β cells	glucose
	Glut 8	testis, brain, fat, liver, and spleen	glucose, fructose
	Glut 10	heart and lung	glucose, galactose
	Glut 12	insulin-sensitive tissues	glucose, galactose, fructose
	Glut 13	Brain	myoinositol

1.2 GLUTs: Structure and Mechanism of Function

GLUT structures are highly conserved and are typically two bundles of six transmembrane helixes (TM) with four to five intercellular helixes (IC) for stabilization [16, 17]. GLUTs rely on a concentration gradient to transport substrates; it is based on substrates moving from an area of high concentration (typically outside the cell) into an area of low concentration (typically inside the cell). Transportation begins with outward-open conformation of GLUTs, and a substrate binds substrate active site. Once key residues have been bound, interactions between TMs trigger a conformational change within the transporter that orients the substrate to the endofacial binding site. Once deposited into the cell, the substrate can be effectively excreted via the same pathway. However, in the conditions of sufficient carbohydrate phosphorylation, carbohydrate excretion is believed to play an insignificant role in evaluating the kinetics of the uptake [18-20], because GLUT transporters being antiporter take up and excrete carbohydrates, but not their phosphorylated analogs [21]. As a result, sugar transport is loosely coupled to phosphorylation, so that a high rate of sugar accumulation is maintained without requiring a reduction in the intracellular sugar concentration.

1.2.1 Class I: GLUTs 1-4

GLUT1 is the most widely studied and targeted of the GLUT transporters and is currently the key target in Positron Emission Topography (PET) imaging using a F^{18}-labelled glucose and is widely used throughout the world as a potent cancer imaging agent. GLUT1 has twelve transmembrane (TM) segments split into two six-helix bundles carboxy- and amino- domains (C and N respectfully). The transporter

preferentially sits in an exofacial conformation stabilized by inter-TM salt bridges on the endofacial side of the transporter that are not present in the endofacial-open conformation of the transporter. When glucose enters the binding site increased interactions between C and N domains and with a protonation of Asp126 leads to cation-π interaction with the aromatic Tyr292 residue causes the transporter to adopt the intercellular conformation. With the release of the substrate via concentration gradient interactions between C and N residues equilibrate and with a deprotonation returns to the original extracellular state [16].

Central cavity of GLUT1 encompasses a multitude of residues including Phe26, Gln166, Ile169, Ile173, Gln287, Gln288, Asn324, Phe379, Gly384, Trp388, Asn411, and Trp419, with most of these residues residing on the C-terminal of the protein leading to asymmetrical binding site [17]. Understanding what is necessary for binding and what can be tolerated to initiate transport is vital for designing anything from probes to cytotoxic therapies for GLUT1. To determine the vital interactions, a large series of structural activity relationship (SAR) studies have been conducted. Early studies have shown that GLUT1 has a highly effective in transporting D-glucose while struggles to transport L-glucose, suggesting the transport to be sensitive towards stereochemistry of the glucose hydroxyls [22]. In agreement with these observations, glucose anomers have shown a loss in the uptake efficiency. Poor uptake was also documented for glucose analogs bearing alkoxy groups. Contrary to effects observed by removal of the C2 and C9 hydroxyls which did not impact the uptake of glucose, with resulting 2-deoxy and 6-deoxy-D-glucose competing for uptake with D-glucose [23]. Building upon these findings 2-chloro and 2,2'-dichlor-2-deoxy-D-glucose were

found to have similar binding affinity to D-glucose, suggesting C2 position may serve

Table 2. Structure-Uptake relationship of GLUT uptake

Substrate	Transport Rate, (%)			
	Glut1[a]	Glut2[b]	Glut3[b]	Glut4[b]
Controls				
D-glucose	1	20±6	10±2	12±3
L-glucose	95	100	100	100
***C*1 Analogs**				
1-Deoxy-D-glucose	82	109±10	104±12	79±12
***C*2 Analogs**				
2-Deoxy-D-glucose	1	20±2	12±2	14±9
D-Mannose	33	29±3	14±2	13±7
2-Chloro-D-glucose	n.d.	76±5	42±3	40±7
***C*3 Analogs**				
3-O-Methyl-D-glucose	30	73±6	17±3	41±7
3-O-Propyl-D-glucose	n.d.	100±12	80±7	72±8
3-Deoxy-D-glucose	67	103±12	85±7	106±12
3-Bromo-D-glucose	n.d.	95±10	75±4	79±12
3-Fluoro-D-glucose		85±5	14±2	40±6
D-Allose	75	59±6	96±7	96±7
***C*4 Analogs**				
D-Galactose	48	110±12	57±5	96±12
***C*5/*C*6 Analogs**				
6-Deoxy-D-glucose	8	33±9	46±7	44±7
D-Xylose	n.d.	106±9	78±6	75±6
L-Arabinose	n.d.	138±22	63±7	90±8
6-O-Methyl-D-galactose	95	57±10	109±11	59±6
6-Fluoro-D-galactose	n.d.	50±12	30±9	48±12

Transport rate determined relative to the uptake of [a]D-[^{3}H]-glucose; [b][2,6-^{3}H]-2-deoxyglucose;n.d., not determined.

as an accommodating position for payload conjugation.

Continues testing has revealed that glucose recognition is highly dependent on the C1-OH as an H-bonding acceptor and the binding has been suggested to work in tandem with hydrophobic interactions on the C6 position. C1 methylation, removal or substitution (with exception of 1-fluoro-D-glucose) all demonstrated exceptional loss of uptake [9, 23, 24]. Although removing C6 hydroxyl still permitted glucose transport, any significant bulk on the position reduced transporter affinity. Overall SAR studies have identified C1, C3 and C4 hydroxyls and C6 hydrophobic interactions are critical points for glucose binding to the active site in GLUT1.

GLUT2, 3 and 4 share many key H-bonding interactions when transporting glucose as GLUT2 and 3 require the presence of C1, C3 and C4 hydroxyls for effective glucose transport [11]. Like with GLUT1 C2 substitution was tolerated but did negatively impact uptake with GLUT2 being the most sensitive to this alteration. GLUTs 2-4, unlike GLUT1, are not glucose specific and have been found to transport D-mannose as efficiently as D-glucose. GLUT1 and 3 can effectively transport 3-fluoro-D-glucose but GLUT2 being unable, pointing towards a C3-OH H-donating effect not required in GLUT3 or 4 [10]. Both GLUT2 and 4 can transport O-6-methyl-D-galactose, but GLUT3 shows little to no affinity. All three can transport the 6-fluoro analog hinting towards extended hydrophobic interactions required in GLUT2 and GLUT4 while GLUT3 has a low tolerance for any steric interactions. Although no crystal structures of GLUT2-4 it is likely that they share similar structures however it is difficult to know if they have more or less TM or ICH.

1.2.2 GLUT5

Class II transporter GLUT5 is the only known transporter that specifically transports fructose and nothing else. In conjunction with GLUT2, they are responsible for most of the fructose transport in the human body [27]. GLUT5 has been a topic of increasing interest in recent years as it has been found to be overly active in breast cancer, while at relatively inactive levels in normal breast cells [28]. Unlike most GLUTs, GLUT5 has had a crystal structure released (Figure 2) and has shown large conservation between GLUT1 but with some key differences. Like GLUT1 it is two bundles of six transmembrane helixes however it has five intercellular helixes that are key for stabilization. Inter-TM salt bridges are a common stabilizing force in major facilitator superfamily transporters and are present only while GLUT5 is in the outward-facing conformation. The observed salt bridges are formed between C-terminal helixes TM3, 4 and 5 and form between N-terminal helixes TM9, 10 and 11. Glu151 (TM4) forms two salt bridges between two arginine residues: Arg97 (TM3) and Arg407 (TM11) whereas Glu400 (TM10) also binds to Arg158 (TM5) and Arg340 (TM9) to complete a stable network between the two terminals.

When GLUT5 transitions to the inward-open conformation, no C-N terminal salt bridges are observed, and the conformational change in the transporter facilitates the entering and exiting of the substrate. Further indicating a preference to outward-open is the linking of Glu252 (ICH3) forming salt bridges with Arg407 (TM11), which is broken upon the inward-open conformation. The most important transitions that take place in GLUT5 occur in TM7 and TM10 as both undergo dramatic shifts to facilitate a conformational change. TM7 shifts down towards the binding site as substrate enters the central cavity whereas TM10 moves away from the binding site breaking the strong

interactions of Tyr382 (TM10) and Ile295 and Val292 (TM7) and allowing fructose transport. These observations suggest TM7-TM10 interactions play an integral role in transport kinetics [17].

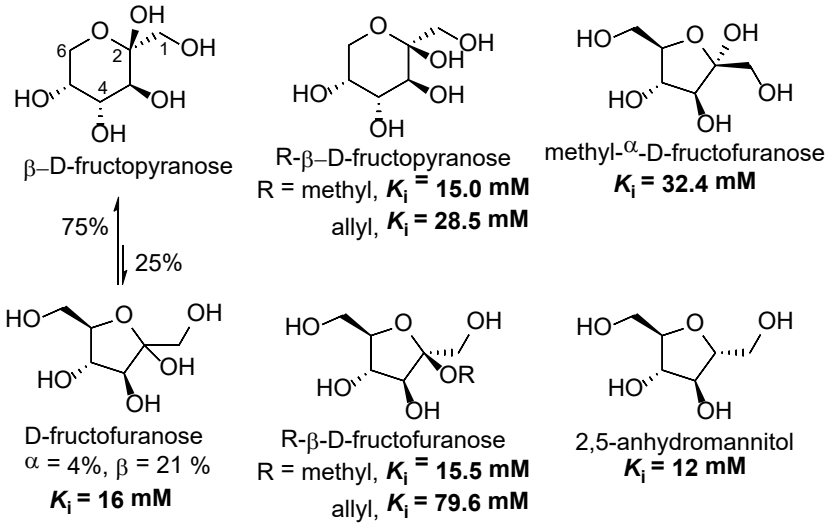

Figure 1.1: Comparison of interaction of C2-derivatives of furanose and pyranose ring forms of fructose with GLUT5. Inhibitory constants were derived by monitoring inhibitory effect of analogs on the uptake of [^{14}C]-D-fructose into CHO cells expressing Glut5.

The binding site for fructose has been extensively studied by Holman et al. [13, 29-31], and determined that stereochemistry and presence of hydroxyls be vital to substrate uptake (Figure 1.1). GLUT5 mediated fructose uptake was found to prefer beta-anomers over alpha-anomers determined by testing C2-methylated fructopyranose and fructofuranose analogs [13]. Alterations of stereochemistry of ring hydroxyls or alkylation was found to dramatically limit affinity to GLUT5 with the notable exception of the C2 position. When 2,5-anhydro-D-mannitol was tested it revealed that the anomeric hydroxyl plays little to no role in GLUT5 fructose transport and that GLUT5 effectively takes up fructose in its furanose form as opposed to its pyranose form [29]. Cyclic oxygen has been found to be vital for uptake via GLUT5 as thio-

substitution led to six-fold loss of uptake was observed [32]. C2 and C5 stereocenters were found to increase uptake during an *anti*-relationship when comparing 2,5-anhydro-D-mannitol uptake vs. L-sorbose (Figure 1.2).

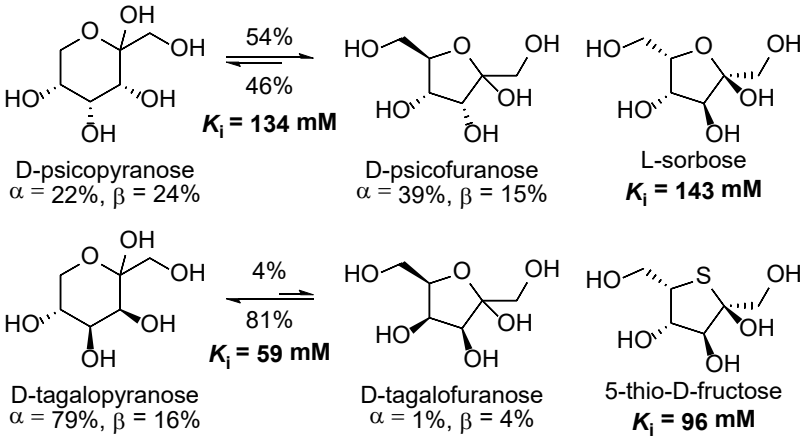

Figure 1.2: Conformer ratios and inhibitory constants for fructose uptake via GLUT5 for D-fructose, D-psicose, and D-tagatose.

The Holman team envisioned a locked series of analogs may provide key insight in GLUT5 binding and potentially series of GLUT5 specific probes (Figure 1.3). These probes were split into type I and type II and differed in existence of the C1 hydroxyl with type I maintaining while type II removed. Type I scaffolds were tested to inhibit D-fructose uptake in the presence of both C1 hydroxyl and ether and was found to inhibit uptake in both cases [31]. In the presence of a carbonyl, oxazolidine uptake was nearly 4-fold higher than its thio counterpart pointing towards key oxygen interaction with the transporter. Type II analogs failed to inhibit D-fructose uptake regardless of stereochemistry, indicating that C1 and C6 oxygens are vital for transport in GLUT5, but C1 acts primarily as an H-bond acceptor or a similar coordination with the transporter. These studies in conjunction with crystal structure have given a good image on what GLUT5 will tolerate to induce binding, but severe limitations persist in

understanding size and functionalization of payloads that transporter permits to pass through.

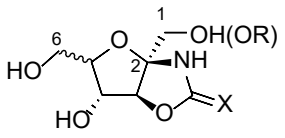

I

Derivatives of	K_i, mM	
D-fructose (R = H)	25 (X = S),	12 (X = O)
D-fructose (R = Bn)	32	9
L-sorbose (R = H)	17	7
L-sorbose (R = Bn)	12	3

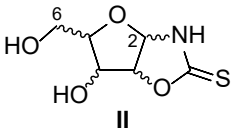

II

Derivatives of	K_i, mM
L-arabinose	123
D-arabinose	104
D-xylose	106
D-ribose	109

Figure 1.3: Bicyclic furanose analogs testing GLUT5 uptake conditions

1.3 GLUTS in Therapy

As discussed previously, PET imaging is one of the most successful utilization of overactive GLUT transport in diseased cells (mainly cancer), but it is not the only one currently in use and development. Quantifying transporters in the membrane has several limitations and involve time-consuming experiments such as western blots or extensive mutagenesis. Monitoring carbohydrate mimics uptake gives a quick and telling analysis of relative expression and activity of transporters that are being specifically targeted.

1.3.1 Carbohydrates as diagnostic probes

The apparent relationship between deregulated carbohydrate uptake/metabolism and disease has triggered interest in GLUT-targeting diagnostic probes. SAR and kinetic analysis of various substrates (described above) have led to the development of radiolabeled probes as well as fluorescent analytical probes. The understanding that C2 and C6 hydroxyls do not play a role in the uptake provided handles for halogenated analogs to act as radiotracers to measure glucose uptake in

diseases. 2-Deoxy-D-glucose (FGD) was first reported by Pacak and co-workers in 1968 [33], and the first ^{18}F-labeled analog (^{18}F-FGD, **1**, Figure 6) was reported by Brookhaven National Laboratory in 1978 [34]. ^{18}F-FDG is rapidly transported into a cancerous cell due to its increased metabolism and undergoes phosphorylation to prevent excretion. Increased intracellular accumulation of ^{18}F-FDG in cancerous cells provides key insight into important cancer characteristics namely enhanced glucose transport as well as enhanced phosphorylation. ^{18}F-FDG has seen wide use as a predictor of tumorigenesis [35-39]. However, it is ineffective with a large number of cancers (including breast cancers) that have reduced glucose uptake capacity [2, 40], and produces false-positive hits due to accumulation at the of inflammation [41, 42].

Due to limitations of FDG needing to be phosphorylated to remain in the cell to accurately measure glucose transport independent of cellular phosphorylation. [^{123}I]-6-deoxy-6-iodo-D-glucose (6DIG, **2**, Figure 1.4) was first synthesized by Wassenaar to act as a tracer unaffected by phosphorylation [43]. Biological studies of 6DIG performed by Henry and co-workers [44] confirmed that 6DIG underwent cellular transport via GLUTs without phosphorylation making it a valuable tool in tracing glucose transport. *In vitro* studies involving adipocytes of diabetic rats and obese mice indicated 6DIG as a potential tool for determining glucose transport derivations in diseases [45]. 6DIG was found to undergo preferential uptake in adiposities, and cardiac cells, both with have high concentrations of insulin-regulated GLUT4 and was proposed as a potential *in vivo* tool to measure insulin resistance. Using diabetic mice and insulin-resistant fructose-fed rats, Perret, and coworkers [46-48] determined glucose transport defects *in vivo* using 6DIG.

Class II fructose specific transporter GLUT5 has gained considerable attention as a potential cancer target due to its alleged role in cancer development [7]. Designed by Maeda and co-workers [49], 1-[^{18}F]-Fluoro-1-deoxy-D-fructose (**3**, Figure 1.4) acted as a tracer in to specifically target GLUT5. Synthesized in two steps from 2,3,4,5-di-*O*-iso-propilidene-1-*O*-(trifluoromethane sulfonyl)-D-fructose, 1-[^{18}F]-Fluoro-1-deoxy-D-fructose rapidly passed through kidney and liver when tested in rat and mouse tumor grafts. Development of 6-fluoro-6-deoxy-D-fructose (**4**, Figure 1.4) [38, 50], found a tracer capable of entering murine EMT-6 and the human breast cancer MCF cells. 6-[^{18}F]-FDF acted as hexokinase substrates and was rapidly metabolised *in vivo*.

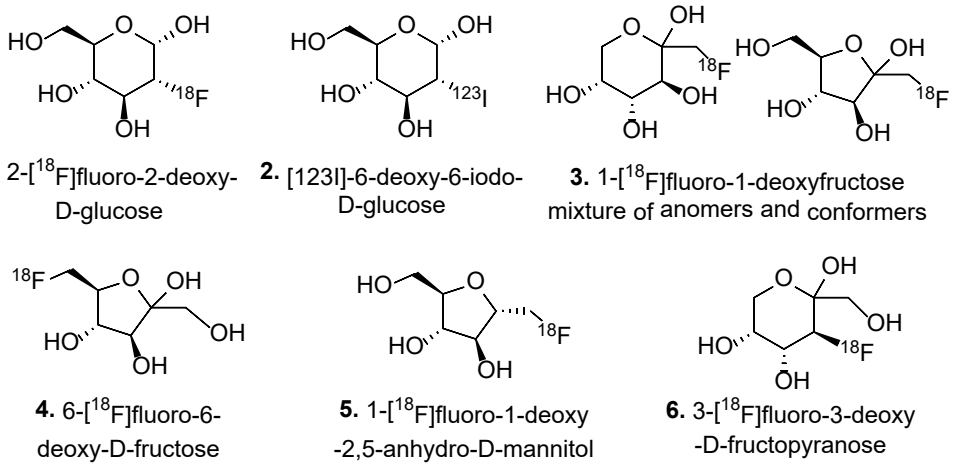

Figure 1.4: Glucose and fructose-based PET imaging probes

The next generation of radiotracer probes was derived from 2,5-anhydro-D-mannitol based on its high affinity towards GLUT5. Niu tested PET imaging agent [39] 1-[^{18}F-fluoro]-1-deoxy-2,5-anhydro-D-mannitol [51] (**5**, Figure 1.4) in breast cancer solid tumours. Results displayed rapid excretion after internalization by cancerous cells requiring optimization to increase retention. 3-(^{18}F)fluoro-3-deoxy-D-fructose (**6**, Figure 1.4) developed by Cheeseman et al. [52] showed fructose specific transport by

a series of competitive uptake inhibition studies and was shown to enter multiple cancer cells lines including EMT-6, CHO, and MCF. Although not as successful as glucose PET imaging tracer, preliminary results have warranted development of more stable and easily retained fructose analogs for PET imaging in the future.

1.3.2 Carbohydrates in chemotherapy

Glycoconjugation provides a potentially elegant way of preferentially targeting cancerous cells in the presence of normal, healthy cells by targeting the overactive metabolism of cancer [14]. Glufosfamide (**8**, Figure 1.5) acted as a prodrug, remaining inactive until cleavage of the glucose after endocytosis into the cell and was one of the first glycoconjugated drugs used [14]. Glufosfamide failed to pass phase II clinical trials for unknown reasons, however, did specifically target glucose transport and provided a potential starting point. Glycoconjugation has been used in an attempt to increase specificity for existing drugs such as chlorambucil which was conjugated to several sugars in an attempt to improve specificity and cytotoxicity [53]. Chlorambucil was conjugated with 63 compounds including glucose (**7**, Figure 1.5), mannose, galactose, and xylose, and conjugation were shown to improve cytotoxicity up to 8-fold [54]. It is unknown if chlorambucil's increased cytotoxicity was caused due to a GLUT-transport or increased accumulation in the cell due to sugar conjugation but it is a likely hypothesis. Conjugates were not limited to chlorambucil and have been developed for the following (not limited to) anticancer agents: azinomycin, clioquinol, adriamycin, warfarin, cyclopamine, 8-[O^6-(4-bromothenyl)-guanine, quinolinyl and methane sulfonate, and paclitaxel (Taxol), with varying success [14].

Lactate dehydrogenase (LDH) inhibitors [55] were developed with the intention of selectively target tumors and act as a photosensitizer [56]. LDH inhibitor N-hydroxy indole (NHI) (**9**, Figure 1.5) [55] conjugated of glucose or mannose lead to a noticeable increase (4.5-fold) in antiproliferative effect as well as a similar increase in inhibiting LDH. Likewise, glucose conjugates of 5,10,15,20-tetrakis-2,3,5,6-tetrafluorophenyl-2,3-(methanol(N-methyl) iminomethano) chlorin (**10**, Figure 1.5) were developed with the intention of being a selective and more potent cytotoxic drug (H_2TFC-S-Glc). H_2TFC-S-Glc did show more potency than other photosensitizers but remained non-specific, this is likely due to the substitution of the anomeric hydroxyl (shown previously to be vital for binding) and points to non-GLUT mediated uptake behind the loss of specificity.

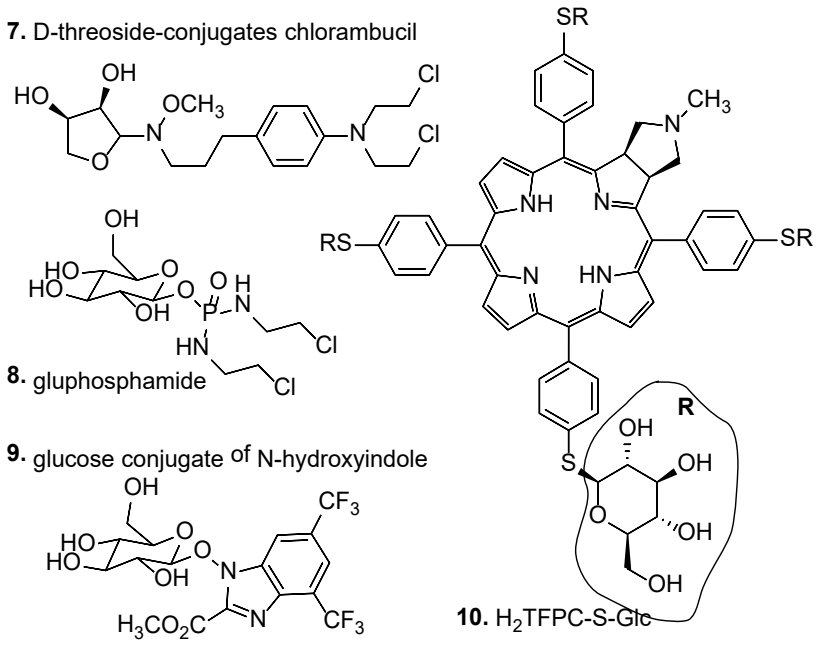

Figure 1.5. Carbohydrates as cancer-directing encore in drug delivery

Platinum (Pt) and palladium (Pd) complexes have seen incredible success in cytotoxicity, but due to lack of specificity lead to horrific side effects, glycoconjugation was attempted to increase specificity in a number of complexes. Tanaka et al. [57] have tested *C*2-Pt and *C*2-Pd glucose conjugates *in vivo* on gastric cancer cells that have been shown to be cisplatin-sensitive and cisplatin-resistant. Like typical cisplatin, apoptosis was induced by coordination between grooves of the DNA and preventing DNA replication. However, both compounds were found to be less effective and no more specific than typical cisplatin. It is unknown whether the compounds were transported via GLUTs or through some other process and the glucose may have caused steric issues with coordination in DNA to decrease activity.

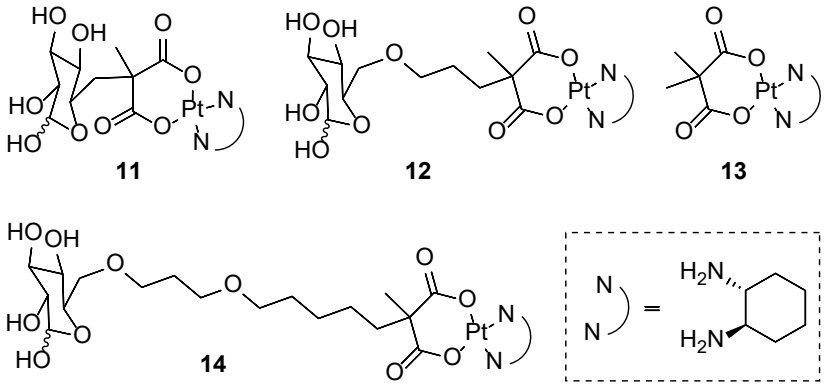

Figure 1.6. Glucose as a delivery platform for platinum compounds.

Lippard, and coworkers [58] were able to identify GLUT preference of C1 and C2 conjugation of Pt and Pd derivatives after screening several isomers. These results agree with previous observations studies [9, 24]. In a separate studies, Lippard and coworkers have designed and evaluated C6-Pt conjugates (**11-14**, Figure 1.6) that differed in the linker length between Pt and the carbohydrate.[59] Using bacterial xylose transporter XylE, which is very similar to GLUT1, molecular docking studies

showed conjugates undergoing H-bonding interactions with key residues Gln288, Gln168, Gln175 and Tyr298 pointing towards GLUT-mediated uptake.

4,6-*O*-ethylidene-α-D-glucose (EDT) in the presence of conjugates **11**-**14** was found to inhibit uptake indicating GLUT1 as the route for intercellular uptake and was found to decrease as linker length was increased [60]. Aglycone **13** was found not undergo GLUT-mediated uptake and likely go through passive diffusion [59]. Pt-glucose conjugates were found to have similar cytotoxicity of aglycone **13** and higher than cisplatin in a number of human cancer cells. Cytotoxicity was experienced after shorter incubation periods indicating the difference in kinetics between facilitative GLUT transport vs. that of passive diffusion that aglycone and cisplatin rely on. The compounds **11** and **12** were found to platinate DNA leading to cell apoptosis, with the number of platinated residues relatively similar to oxaliplatin. The uptake of **11**-**14** was also found to different extend to depend on the organic transporter 2 (OCT2, involved in the uptake of **14**), with **11** showing more GLUT-specific uptake that other analogs. Further evaluation showed **11** to be more cytotoxic in cancer vs. normal cells, giving a good platform for further development of cancer-specific therapeutic agents.

Glycoconjugation has also been used in an attempt to increase selectivity for a variety of other nonspecific methods of drug delivery. Nanoparticles have been widely studied as potent delivery systems for highly cytotoxic payloads but suffer from lack of specificity [61]. In an attempt to increase specificity glycoconjugation with nanoparticles has been attempted with varying success [62]. Li and co-workers [62] developed glucose-conjugated chitosan nanoparticles in an attempt to encapsulate doxorubicin with limited success. Doxorubicin-loaded nanoparticles entered 4T1

cancer cells up via GLUTs and were four times more cytotoxic than non-glucose-conjugated nanoparticles [63].

Glycoconjugation has not been limited to just cancer and has found success in delivering payloads through the blood brain barrier due to high amounts of GLUT1 [64, 65] as well as other barrier structures in the brain [66]. A successful example was ibuprofen-glucose conjugation resulting a dramatic increase in drug delivery to the brain with a three-fold increase in concentration [15]. The massive challenges BBB penetration and water solubility represent for most small molecule drugs prodrug development with glucose provides an elegant solution to both of these issues and represents potentially effective drug delivery system for future drugs [67].

1.3.3 Fluorescent GLUT Probes

Targeting GLUTs has been attempted a variety of fluorescent conjugates. However, the only fluorophore found to pass through GLUTs was green-fluorescent 7-nitrobenzofurazan (NBD). Conjugation of amino sugars – 2-Amino-2-deoxy-D-glucose (G) [68], 1-deoxy-1-amino-D-fructose (F) [69], and 1-amino-2,5-anhydro-D-mannitol (M) [70] with NBD has produced a probes specific for certain GLUTs (Figure 1.7).

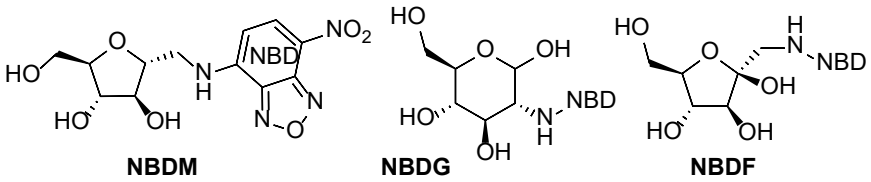

Figure 1.7: Green fluorescent GLUT-targeting probes

NBDG is glucose dependent [68, 71], and is likely passes through most class I transporters. NBDF uptake is facilitated by glucose- and fructose-transport and is

likely to rely on GLUT2 and GLUT5 [69]. MNBD uptake depends only on fructose and likely passes specifically through GLUT5, suggesting some preference of the transporter towards the locked furanose ring. Altogether, NBDG, NBDF, and NBDM allow assessing the efficiency of glucose-specific transport, non-specific transport and fructose-specific transport, respectively, providing convenient tools for quick analysis of carbohydrate transport efficiency in various cells. All three probes were found to be phosphorylated inside the cell, ensuring their cellular accumulation and retention [72]. Limited attempts to produce red fluorescent probes by conjugating carbohydrate to cianine5 (Cy5) dye resulted in a loss of GLUT-mediate uptake [69], leaving room for further evaluation of transporter preferences in substrate selection. Fluorescent probes have wide room for improvement as NBD competes with auto-fluorescence of cells in the green region and various colors provide an opportunity of tracking various transporters activity simultaneously.

This thesis work focuses on our attempts to develop fructose uptake dependent fluorescent probes. Synthesis and probe design will be discussed in **Chapter 2** while cellular studies will be discussed in **Chapter 3**. Future research plans for additional probes and cancer types will be summarized in **Chapter 4**.

References

1. Marger, M.D. and M.H. Saier, Jr., *A major superfamily of transmembrane facilitators that catalyse uniport, symport and antiport.* Trends Biochem. Sci., 1993. **18**(1): p. 13-20.
2. Manolescu, A.R., et al., *Facilitated hexose transporters: new perspectives on form and function.* Physiology, 2007. **22**: p. 234-40.
3. Isabel Garcia-Alvarez, L.G.a.A.F.-M., *Studies on the Uptake of Glucose Derivatives by Red Blood Cells.* ChemMedChem, 2007: p. 496-504.
4. Liu, L., et al., *Three-dimensional dynamic culture of pre-osteoblasts seeded in HA-CS/Col/nHAP composite scaffolds and treated with alpha-ZAL.* Acta Biochim Biophys Sin (Shanghai), 2012. **44**(8): p. 669-77.
5. Brockmann, K., *The expanding phenotype of GLUT1-deficiency syndrome.* Brain Dev., 2009. **31**(7): p. 545-552.
6. Adekola, K., S.T. Rosen, and M. Shanmugam, *Glucose transporters in cancer metabolism.* Curr. Opin. Oncol., 2012. **24**(6): p. 650-654.
7. McQuade, D.T., M.B. Plutschack, and P.H. Seeberger, *Passive fructose transporters in disease: a molecular overview of their structural specificity.* Org. Biomol. Chem., 2013. **11**(30): p. 4909-4920.
8. Stein, W.D., *The mechanism of sugar transfer across erythrocyte membranes.* Ann. N.Y. Acad. Sci., 1972. **195**: p. 412-28.
9. Barnett, J.E., G.D. Holman, and K.A. Munday, *Structural requirements for binding to the sugar-transport system of the human erythrocyte.* Biochem. J., 1973. **131**(2): p. 211-221.

10. Colville, C.A., M.J. Seatter, and G.W. Gould, *Analysis of the Structural Requirements of Sugar Binding to the Liver, Brain and Insulin-Responsive Glucose Transporters Expressed in Oocytes.* Biochem. J., 1993. **294**: p. 753-760.
11. Colville, C.A., et al., *Kinetic-Analysis of the Liver-Type (Glut2) and Brain-Type (Glut3) Glucose Transporters in Xenopus Oocytes - Substrate Specificities and Effects of Transport Inhibitors.* Biochem. J., 1993. **290**: p. 701-706.
12. Nishimura, H., et al., *Kinetics of Glut1 and Glut4 Glucose Transporters Expressed in Xenopus Oocytes.* J. Biol. Chem., 1993. **268**(12): p. 8514-8520.
13. Tatibouet, A., et al., *Synthesis and evaluation of fructose analogues as inhibitors of the D-fructose transporter GLUT5.* Bioorgan. Med. Chem., 2000. **8**(7): p. 1825-1833.
14. Calvaresi, E.C. and P.J. Hergenrother, *Glucose conjugation for the specific targeting and treatment of cancer.* Chem. Sci., 2013. **4**(6): p. 2319-2333.
15. Chen, Q., et al., *Synthesis, in vitro and in vivo characterization of glycosyl derivatives of ibuprofen as novel prodrugs for brain drug delivery.* J. Drug Target., 2009. **17**(4): p. 318-328.
16. Deng, D., et al., *Crystal structure of the human glucose transporter GLUT1.* Nature, 2014. **510**(7503): p. 121-5.
17. Nomura, N., et al., *Structure and mechanism of the mammalian fructose transporter GLUT5.* Nature, 2015. **526**(7573): p. 397-401.
18. Naftalin, R.J. and R.J. Rist, *Evidence That Activation of 2-Deoxy-D-Glucose Transport in Rat Thymocyte Suspensions Results from Enhanced Coupling*

between Transport and Hexokinase-Activity. Biochem. J., 1989. **260**(1): p. 143-152.

19. Naftalin, R.J. and P.M. Smith, *A Model for Accelerated Uptake and Accumulation of Sugars Arising from Phosphorylation at the Inner Surface of the Cell-Membrane.* Biochim. Biophys. Acta, 1987. **897**(1): p. 93-111.
20. Gasbjerg, P.K. and J. Brahm, *Glucose-Transport Kinetics in Human Red-Blood-Cells.* Biochim. Biophys. Acta, 1991. **1062**(1): p. 83-93.
21. Azema, L., et al., *Interaction of substituted hexose analogues with the Trypanosoma brucei hexose transporter.* Biochem. Pharmacol., 2004. **67**(3): p. 459-467.
22. Kahlenberg, A., B. Urman, and D. Dolansky, *Preferential uptake of D-glucose by isolated human erythrocyte membranes.* Biochemistry, 1971. **10**(16): p. 3154-3162.
23. Rees, W.D. and G.D. Holman, *Hydrogen-Bonding Requirements for the Insulin-Sensitive Sugar-Transport System of Rat Adipocytes.* Biochim. Biophys. Acta, 1981. **646**(2): p. 251-260.
24. Kahlenberg, A. and D. Dolansky, *Structural requirements of D-glucose for its binding to isolated human erythrocyte membranes.* Can. J. Biochem., 1972. **50**(6): p. 638-43.
25. James, D.E., et al., *Insulin-Regulatable Tissues Express a Unique Insulin-Sensitive Glucose-Transport Protein.* Nature, 1988. **333**(6169): p. 183-185.
26. Stenbit, A.E., et al., *GLUT4 heterozygous knockout mice develop muscle insulin resistance and diabetes.* Nature Medicine, 1997. **3**(10): p. 1096-1101.

27. Douard, V. and R.P. Ferraris, *Regulation of the fructose transporter GLUT5 in health and disease.* Am J Physiol Endocrinol Metab, 2008. **295**(2): p. E227-37.

28. Zamora-Leon, S.P., et al., *Expression of the fructose transporter GLUT5 in human breast cancer.* Proc. Natl. Acad. Sci. U.S.A., 1996. **93**(5): p. 1847-52.

29. Yang, J., et al., *Fructose analogues with enhanced affinity for GLUT5.* Diabetes, 2001. **50**: p. A277-A277.

30. Yang, J., et al., *Development of high-affinity ligands and photoaffinity labels for the D-fructose transporter GLUT5.* Biochem. J., 2002. **367**: p. 533-539.

31. Girniene, J., et al., *Inhibition of the D-fructose transporter protein GLUT5 by fused-ring glyco-1,3-oxazolidin-2-thiones and -oxazolidin-2-ones.* Carbohyd. Res., 2003. **338**(8): p. 711-719.

32. Tatibouet, A., et al., *D-Fructose-L-sorbose interconversions. Access to 5-thio-D-fructose and interaction with the D-fructose transporter, GLUT5.* Carbohyd. Res., 2001. **333**(4): p. 327-334.

33. Pacak, J., Z. Tocik, and M. Cerny, *Synthesis of 2-Deoxy-2-fluoro-D-glucose.* Chem. Commun., 1969: p. 77-77.

34. Ido, T., et al., *Labeled 2-Deoxy-D-Glucose Analogs - F-18-Labeled 2-Deoxy-2-Fluoro-D-Glucose, 2-Deoxy-2-Fluoro-D-Mannose and C-14-2-Deoxy-2-Fluoro-D-Glucose.* J. Labelled Comp. Rad., 1978. **14**(2): p. 175-183.

35. Larson, S.M., *Positron emission tomography-based molecular imaging in human cancer: exploring the link between hypoxia and accelerated glucose metabolism.* Clin. Cancer Res., 2004. **10**(7): p. 2203-2204.

36. Machtay, M., et al., *Prediction of Survival by [18F]Fluorodeoxyglucose Positron Emission Tomography in Patients With Locally Advanced Non-Small-Cell Lung*

Cancer Undergoing Definitive Chemoradiation Therapy: Results of the ACRIN 6668/RTOG 0235 Trial. J. Clin. Oncol., 2013. **31**(30): p. 3823-3830.

37. Wahl, R.L., et al., *18F-2-deoxy-2-fluoro-D-glucose uptake into human tumor xenografts. Feasibility studies for cancer imaging with positron-emission tomography.* Cancer, 1991. **67**(6): p. 1544-1550.
38. Wuest, M., et al., *Radiopharmacological evaluation of 6-deoxy-6-[F-18]fluoro-D-fructose as a radiotracer for PET imaging of GLUT5 in breast cancer.* Nuc. Med. Biol., 2011. **38**(4): p. 461-475.
39. Niu, B., et al., *Synthesis and Preliminary Evaluation of 1-[F-18]Fluoro-1-deoxy-2,5-anhydro-D-mannitol as a PET Radiotracer for Breast Cancer Imaging.* Chinese J. Chem., 2013. **31**(9): p. 1159-1163.
40. Kim, J., et al., *Selective Sentinel Node Plus Additional Non-Sentinel Node Biopsy Based on an FDG-PET/CT Scan in Early Breast Cancer Patients: Single Institutional Experience.* World J. Surg., 2009. **33**(5): p. 943-949.
41. Lind, P., et al., *Advantages and limitations of FDG PET in the follow-up of breast cancer.* Eur. J. Nucl. Med. Mol. I, 2004. **31**: p. S125-S134.
42. Alavi, A. and H.M. Zhuang, *Finding infection - help from PET.* Lancet, 2001. **358**(9291): p. 1386-1386.
43. Wassenaar, W. and C.H. Tator, *Glucose analogues as potential agents for brain tumour diagnosis and treatment.* Trans. Am. Neurol. Assoc., 1973. **98**: p. 43-8.
44. Henry, C., et al., *[123I]-6-deoxy-6-iodo-D-glucose (6DIG): a potential tracer of glucose transport.* Nucl. Med. Biol., 1997. **24**(6): p. 527-34.

45. Henry, C., et al., *Characterization of 6-deoxy-6-iodo-D-glucose: a potential new tool to assess glucose transport.* Nucl. Med. Biol., 1997. **24**(1): p. 99-104.

46. Slimani, L., et al., *[Multi-compartmental modelling and experimental design for glucose transport studies in insulin-resistant rats].* C. R. Biol., 2002. **325**(4): p. 529-46.

47. Perret, P., et al., *Assessment of insulin sensitivity in vivo in control and diabetic mice with a radioactive tracer of glucose transport: [125I]-6-deoxy-6-iodo-D-glucose.* Diabetes. Metab. Res. Rev., 2003. **19**(4): p. 306-12.

48. Perret, P., et al., *Assessment of insulin resistance in fructose-fed rats with I-125-6-deoxy-6-iodo-D-glucose, a new tracer of glucose transport.* Eur. J. Nucl. Med. Mol. I., 2007. **34**(5): p. 734-744.

49. Haradahira, T., et al., *Radiosynthesis, rodent biodistribution, and metabolism of 1-deoxy-1-[18F]fluoro-D-fructose.* Nucl. Med. Biol., 1995. **22**(6): p. 719-725.

50. Trayner, B.J., et al., *Synthesis and characterization of 6-deoxy-6-fluoro-D-fructose as a potential compound for imaging breast cancer with PET.* Bioorgan. Med. Chem., 2009. **17**(15): p. 5488-5495.

51. Plutschack, M.B., et al., *Flow synthesis of a versatile fructosamine mimic and quenching studies of a fructose transport probe.* Beilstein J. Org. Chem., 2013. **9**: p. 2022-2027.

52. Soueidan, O.M., et al., *New fluorinated fructose analogs as selective probes of the hexose transporter protein GLUT5.* Org. Biomol. Chem., 2015. **13**(23): p. 6511-6521.

53. Reux, B., et al., *Synthesis and cytotoxic properties of new fluorodeoxyglucose-coupled chlorambucil derivatives.* Bioorg. Med. Chem., 2008. **16**(9): p. 5004-5020.

54. Goff, R.D. and J.S. Thorson, *Assessment of Chemoselective Neoglycosylation Methods Using Chlorambucil as a Model.* J. Med. Chem., 2010. **53**(22): p. 8129-8139.

55. Di Bussolo, V., et al., *Synthesis and biological evaluation of non-glucose glycoconjugated N-hydroyxindole class LDH inhibitors as anticancer agents.* RSC Adv., 2015. **5**(26): p. 19944-19954.

56. Tanaka, M., et al., *Anticancer Effects of Novel Photodynamic Therapy with Glycoconjugated Chlorin for Gastric and Colon Cancer.* Anticancer Res., 2011. **31**(3): p. 763-769.

57. Tanaka, M., et al., *Anti-cancer effects of newly developed chemotherapeutic agent, glycoconjugated palladium (II) complex, against cisplatin-resistant gastric cancer cells.* BMC Cancer, 2013. **13**: p. 237-245.

58. Patra, M., S.G. Awuah, and S.J. Lippard, *Chemical Approach to Positional Isomers of Glucose-Platinum Conjugates Reveals Specific Cancer Targeting through Glucose-Transporter-Mediated Uptake in Vitro and in Vivo.* J. Am. Chem. Soc., 2016. **138**(38): p. 12541-51.

59. Patra, M., et al., *A Potent Glucose-Platinum Conjugate Exploits Glucose Transporters and Preferentially Accumulates in Cancer Cells.* Angew. Chem. Int. Ed., 2016. **55**(7): p. 2550-4.

60. Barnett, J.E., et al., *Evidence for two asymmetric conformational states in the human erythrocyte sugar-transport system.* Biochem. J., 1975. **145**(3): p. 417-29.

61. Yang, K.K., et al., *Preparation and characterization of a novel thermosensitive nanoparticle for drug delivery in combined hyperthermia and chemotherapy.* J. Mater. Chem. B, 2013. **1**(46): p. 6442-6448.

62. Li, J., et al., *Glucose-conjugated chitosan nanoparticles for targeted drug delivery and their specific interaction with tumor cells.* Front. Mater. Sci., 2014. **8**(4): p. 363-372.

63. Yang, K.K., et al., *Preparation and characterization of a novel thermosensitive nanoparticle for drug delivery in combined hyperthermia and chemotherapy.* J. Mater. Chem. B, 2013. **1**(46): p. 6442-6448.

64. Boado, R.J. and W.M. Pardridge, *The Brain-Type Glucose Transporter Messenger-Rna Is Specifically Expressed at the Blood-Brain-Barrier.* Biochem. Biophys. Res. Commun., 1990. **166**(1): p. 174-179.

65. Pardridge, W.M., R.J. Boado, and C.R. Farrell, *Brain-Type Glucose Transporter (Glut-1) Is Selectively Localized to the Blood-Brain-Barrier - Studies with Quantitative Western Blotting and Insitu Hybridization.* J. Biol. Chem., 1990. **265**(29): p. 18035-18040.

66. Farrell, C.L., J. Yang, and W.M. Pardridge, *GLUT-1 glucose transporter is present within apical and basolateral membranes of brain epithelial interfaces and in microvascular endothelia with and without tight junctions.* J. Histochem. Cytochem., 1992. **40**(2): p. 193-199.

67. Pardridge, W.M., *Blood-brain barrier drug targeting: the future of brain drug development.* Mol. Interv., 2003. **3**(2): p. 90-105, 51.

68. Zou, C.H., Y.J. Wang, and Z.F. Shen, *2-NBDG as a fluorescent indicator for direct glucose uptake measurement.* J. Biochem. Biophys. Meth., 2005. **64**(3): p. 207-215.

69. Levi, J., et al., *Fluorescent fructose derivatives for imaging breast cancer cells.* Bioconjugate Chem., 2007. **18**(3): p. 628-634.

70. Tanasova, M., et al., *Fluorescent THF-based fructose analogue exhibits fructose-dependent uptake.* ChemBioChem, 2013. **14**(10): p. 1263-70.

71. Yoshioka, K., et al., *A novel fluorescent derivative of glucose applicable to the assessment of glucose uptake activity of Escherichia coli.* BBA-Gen. Subjects, 1996. **1289**(1): p. 5-9.

72. Yoshioka, K., et al., *Intracellular fate of 2-NBDG, a fluorescent probe for glucose uptake activity, in Escherichia coli cells.* Biosci. Biotech. Biochem., 1996. **60**(11): p. 1899-1901.

Chapter 2

Blue Fluorescent Probes GLUT-Mediated Uptake in Breast Cancer

2.1 Introduction

Carbohydrate uptake in mammalian cells is facilitated by membrane proteins called GLUTs which perform gradient-dependent carbohydrate transport [1, 2]. Expression of GLUTs varies throughout the body and can be viewed as a physiological characteristic of the tissue. Mutations of GLUTs have been linked with several medical conditions [3] while alterations to GLUT activity and regulation are characteristic for the metabolically-compromised cell, including cancer cells [4]. GLUT research has been mainly focused on widespread glucose transporter GLUT1 due to its high activity in various cancers. Recent findings have increased interest in the fructose-specific GLUT5 that appears to be expressed in various cancers, while absent in the corresponding non-cancer tissues [5].

The kinetic analysis of carbohydrate transport via GLUTs led to the development of the transport model that included the binding of the substrate to the extracellular site of the transporter, followed by the conformational change in the enzyme and the translocation of the substrate to the intracellular or endofacial side of the membrane [6]. Initial binding of the substrate to the transporters was found to vary with the structure of a carbohydrate, i.e. to depend on sugar conformation and the presence and stereochemistry of hydroxyls [7-11]. The understanding molecular basis for sugar-transporter interaction facilitated the development of biochemical probes to analyze transport efficiency, and dissect the membrane portion from the total GLUT expression. The latter provides the possibility for cell differentiation based on profiling

The following material is in preparation for submission to a journal for publication.

the membrane GLUTs. GLUT-targeting imaging agents and drugs conjugates are of interest to distinguish and kill metabolically-compromised cells [12], or to penetrate the blood-brain barrier [13]. Therapeutic approaches also include inducing a nutrient deficit in cancers, thus stimulating the development of carbohydrate uptake modulators.

Current knowledge of GLUT-substrate interactions and the transport capacity of GLUTs is currently limited and requires significant study to determine. Conjugation of amino sugars – 2-Amino-2-deoxy-D-glucose [14], 1-deoxy-1-amino-D-fructose [15], and 1-amino-2,5-anhydro-D-mannitol [16] to the fluorescent 7-nitro-2,1,3-benzoxadiazole (NBD) has led to effective GLUT uptake probes. However, the efforts to produce fluorescent conjugates of other colors (Cy5-fluorophore) failed, and GLUT-Cy5 conjugate showed to lose GLUT-mediated uptake [15]. Coumarins are aromatic, blue fluorescent molecules with a similar size to NBD with an easily substituted C4 position to make a multitude of probes. GLUT2 and GLUT5 have been shown to be the two primary transporters responsible for fructose transport but whether they both transport fructose in its pyranose or furanose form remains unclear [17]. In this chapter the synthesis of ManCou1, 2 and 3 as well as their effectiveness as imaging probes in various cancerous and normal cell lines.

2.2 Materials and Methods

Materials and methods: Ethanol (ACS/USP Grade, 190 Proof) was purchased from Pharmaco-Aaper, USA. Sterile DMSO (25-950-CQC, 250mL) was from Cellgro, USA. RPMI-1640, DMEM/, Penicillin/Streptomycin, FBS (Fetal Bovine Serum), Sodium Pyruvate (100 mM), 0/25% Trypsin-EDTA (1X), Hank's buffer, PBS (phosphate

buffered saline solution), and RPMI-1640 were was from Life Technologies, USA. Cholera Toxin, Vibrio cholerae, Type Inaba 569B, Azide Free was from Calbiochem, EMD Millipore, USA. Life Technologies, USA. PBS 1X solution was from Janssen Pharmaceutica, Belgium. LIVE/DEAD® Viability/Cytotoxicity Kit, for mammalian cells was from Invitrogen, USA.

Chemical reagents used for the synthesis were purchased from Aldrich. Column chromatography was performed using SiliCycle silica gel (230-400 mesh). Purification of NBD conjugates for cell studies was performed on Agilent HPLC 1200 Series equipped with fraction collector from Agilent Technologies, using Phenomenex C18 column (Luna 5u C18(2) 100A, 250x4.60 mm, 5 micron) using MeOH:H_2O as a mobile phase. Structural analysis of compounds was carried out with 400 MHz Varian NMR instrument. Spectra are reported in parts per million (ppm) relative to the solvent resonances (δ), with coupling constants (*J*) in Hertz (Hz). UV-vis spectra were recorded on a Cary 100 Bio spectrophotometer from Agilent Technologies. High-resolution molecular mass was obtained with Orbitrap Elite mass spectrometer. UV spectra were obtained with Cary-Bio-100 UV-vis spectrometer. Fluorescence spectra were obtained with a FluoroMax-4 spectrophotometer. 96-well plate analysis of cell fluorescence was carried out with Victor3 fluorescence plate reader (excitation at 385 nm). Confocal images were taken with Olympus FluoViewTM FV1000 using the FluoView software.

Chemical synthesis of ManCou probes: (2*S*,3*S*,4*S*,5*R*)-3,4-dihydroxy-5-(hydroxymethyl)tetrahydrofuran-2-carbaldehyde (1) (1 mmol) and the corresponding *C*4-substituted 7-aminocoumarin (1 mmol) were dissolved in 10 ml of methanol. 0.5 M

HCl was used to adjust the pH to 5.8 followed by addition of $NaCH_3CN$ (1.2 mmol) to the reaction mixture. The solution was stirred at room temperature while the pH was maintained at 5.8 by periodic addition of 0.5 M HCl until the starting material was no longer detectable by TLC. The mixture was then concentrated to a small volume under reduced pressure, and the concentrated residue was separated by the semi-preparative HPLC (Kinet 2.6 u HILIC 100A) using a various proportion of water-MeCN as an eluent. The composition of the final product was confirmed ESI, HRMS, ^{1}H NMR and ^{13}C NMR.[18]

Cell Culture: MCF-7 and MCF-10A cells were seeded from frozen standards purchased from ATCC in 10 cm dishes under standard conditions (37 C^{o}, 5% CO_2 / 90% air). MCF-7 cells grown in RPMI-1640 growth medium supplemented with 10% heat-inactivated fetal bovine serum (FBS) and 1% penicillin/streptomycin both purchased from Thermo-Fisher. MCF10A was grown in DMEM growth media supplemented with 10% heat-inactivated fetal bovine serum (FBS), 1% penicillin/streptomycin, and cholera toxin (100 ng/ml). MCF7 was passaged with trypsin every five days, MCF-10A every ten days with media being changed 24 hours after seeding.

Preparing ManCou solutions: ManCou1 and 2 were dissolved in a solution of 10% DMSO/90% Millipore water for stock solution. ManCou3 was dissolved in 70% DMSO/30% Millipore water for stock solution. All solutions for testing were diluted from stock using Hank's buffer solution purchased from Thermo Fisher.

96-well plate fluorescence studies: At >85% confluence cells were collected and plated in 96-well flat bottom plates (20,000 cells/well) purchased from and allowed to grow for 24 hours. Cells were then washed with warmed (37 C^o) Hank's balanced buffer solution and treated with ManCou fluorescent probes (concentration varies) in Hank's and incubated at 37 C^o and 5% CO_2 for 10 min. After incubation, the probe-containing solution was removed, and cells were washed with warmed Hank's (3 x 100 µL) buffer. Fluorescent data was immediately collected using Victor^3 plate reader and using Wallac^{TM} umbelliferone (excitation 355 nm, emission 460 nm, 1.0 s) protocol. All tests were done in duplicate on each plate.

Inhibition studies: Using 96-well plate method fluorescence of ManCou probes in cells war measure in the presence of varying concentrations of glucose, fructose, glucosamine, MNBD, GNBD, and cytochalasin B. Separately, complete culture media was used to establish the impact of nutrients on ManCou uptake. Cell incubation, washing, and data collection was conducted as stated above.

Confocal fluorescence studies: At >85% confluence cells were collected and plated (20,000) in 35 mm glass-bottom confocal dishes (MatTek) and allowed to grow in their respective growth media for 24 hours. Cells were then washed with warmed (37 C°) Hank's (2 x 1 mL) before being incubated with ManCou solution in Hanks (1 mL, 37 C°, 5% CO_2) for 10 min. After incubation cells were again washed with warmed Hank's (3 x 1 mL) and leaving 1 mL of Hank's for images. Images were taken using Olympus FluoView^{TM} FV1000 using the FluoView software. 60X oil suspended lens cells were used to observe fluorescent activity with the following conditions; filter: DAPI, laser:

405 (45% intensity), excitation: 10 µs/pixel. Z-stacking was done using FluoView software and depth command.

Fructose preconditioning: MCF7 cells, grown in the standard growth medium, were passaged and maintained for ten days in *i)* the standard medium supplemented with fructose (11 mm) to produce fructose-fed MCF7' cell culture, and *ii)* in RPMI-1640 medium supplemented with dialyzed FBS (10%) to produce fructose-deprived MCF" cells culture. The MCF" cells were then maintained for ten days in the standard medium to produce fructose-refed MCF7* culture. The medium was changed 24 h after passaging of cells and every two days.

2.3 Synthesis and Computational Analysis of Mannitolamin-Coumarin Conjugates (ManCou Probes)

Several coumarins differing in the functional groups at the C4 position (Figure 2.1) were chosen to assess the possibility to transport extended aromatic system through GLUTs and test the impact of steric, H-bonding and electronic interactions. ManCou1 (H) represents a plain aromatic system with weakly H-bonding carbonyl group that is not expected to exhibit any interactions with the transporter. ManCou2 (CH_3) acts as a weak electron donating group that appears to increase electron density of coumarin aromatic system and possibly contributes to the enhanced H-bonding capability of the carbonyl group. ManCou3 (CF_3) acts as a strong electron withdrawing group deactivating the aromatic system of coumarin and thus increasing its potential capability of π-acceptor. Additionally, the presence of halogens is known to induce halogen-π interactions within proteins, and CF_3 group, in particular, is capable of

stabilizing interactions with aromatic systems [19, 20]. Thus, H-bonding and aromatic interactions would be expected for ManCou3 within the transporter.

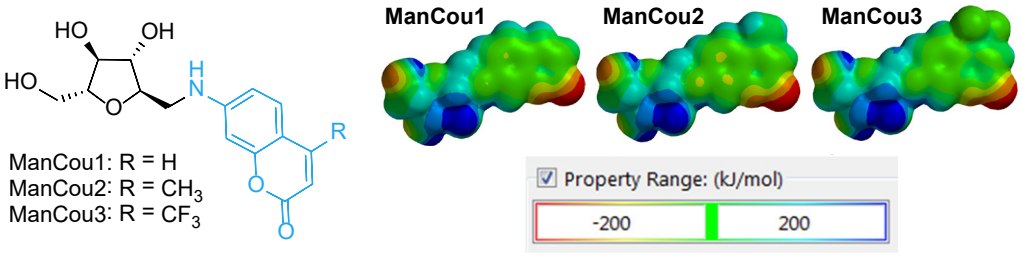

Figure 2.1. ManCou1-3 probes and their electrostatic properties

The synthesis of conjugates was based on the reductive amination of (2*S*,3*S*,4*S*,5*R*)-3,4-dihydroxy-5-(hydroxymethyl) tetrahydrofuran-2-carbaldehyde (**1**) with the corresponding 7-aminocoumarin, resulting in ManCou 1-3 conjugates (Scheme 1). To access aldehyde **1**, D-(+)-glucosamine was carried through a Tiffeneau-Demjanov rearrangement with an acidic resin in the presence of $NaNO_2$ [21]. The aldehyde **1** was isolated in acceptable yield (84%) and was used in the subsequent reactions without purification. The ManCou conjugates were purified by high-pressure liquid chromatography (HPLC) using a gradient of ACN:water and analytical (4.5 Å) C18 reverse phase column (Phenomenex). Structures of ManCou1-3 probes were confirmed with NMR spectroscopy and Mass Spectrometry.

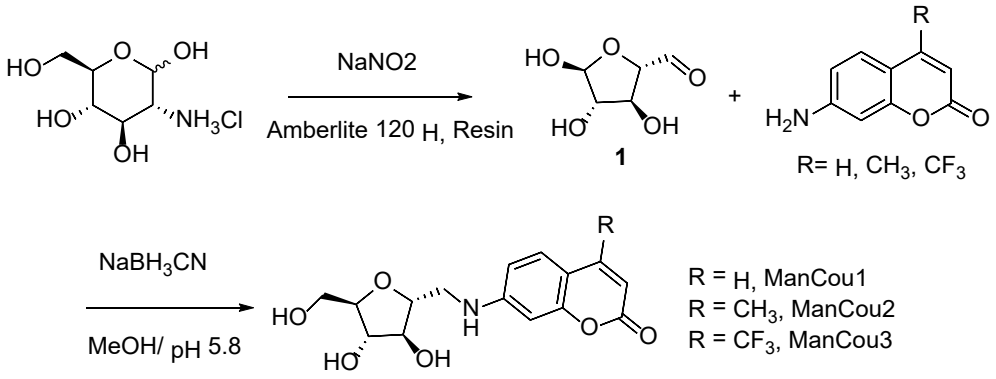

Scheme 2.1. Synthesis of ManCou probes

Optical properties of ManCou1-3 were analyzed through UV-vis (Cary-Bio-100) and fluorescence (FluoroMax-4). The UV and fluorescence (Figure 2.2) spectra for ManCous 1-3 reflected the impact of a methyl- and trifluoromethyl- substituents on the π-system of the fluorophore, with blue- and red-shift observed for ManCou2 and ManCou3, respectively. The relative quantum efficiencies of ManCous 1:2:3 were established as 0.9:1.0:0.30 (determined for 385 nm excitation wavelength). The absolute quantum yields were determined based on the optically matching solution of anthracene [22] (20 μM in ethanol, ϕ = 0.27) as 0.26, 0.30, and 0.10 for ManCou1, ManCou2 and Mancou3 (20 μM in DMSO/H_2O 9:1, v/v), respectively.

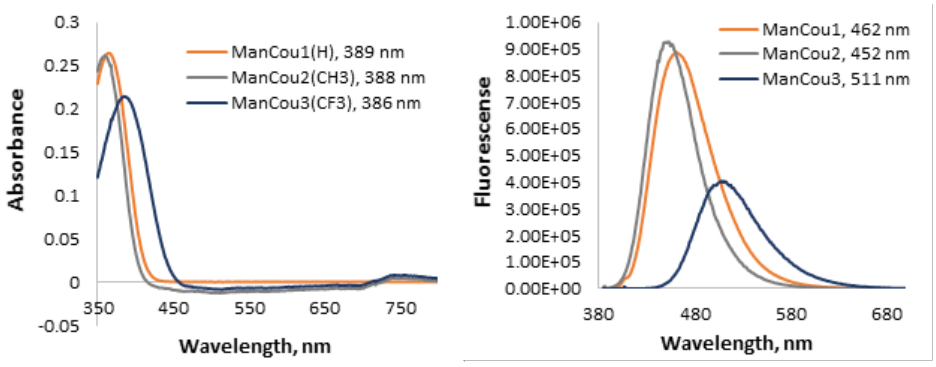

Figure 2.2. UV-vis and fluorescence spectra of ManCou1-3

To gain insight into the ManCou interaction with GLUT5, molecular docking of DFT-optimized structures of coumarin conjugates into the exofacial cavity of a mammalian fructose transporter GLUT5 (PDB code: 4YB9) using Autodock4 [23] was carried out. For each ManCou probe, the resulting complexes were ranked, and the complexes were analyzed to identify the position/binding of conformers.

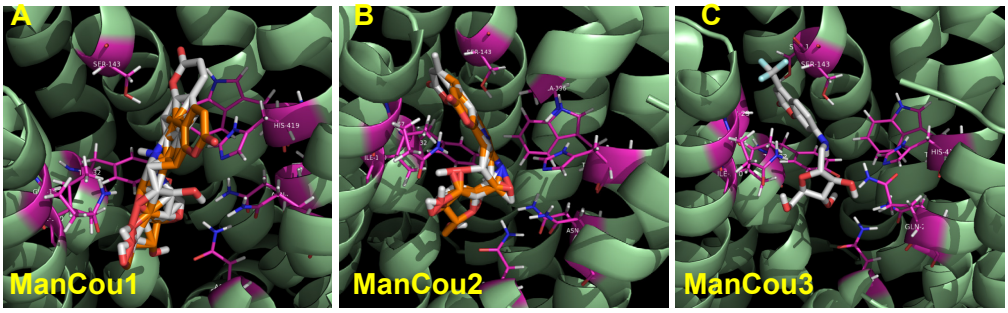

Figure 2.3. Docking analysis of ManCou1-3. Docking analysis performed with Autodock4. Models visualized with PyMol.

Overall, the analysis of complexes showed the ManCous to bind with the uptake relevant residues through the 1-AM moiety but accommodate different orientations of the fluorophore (Figure 2.3). All three probes were found to H-bond with Tyr32, Gln167, Gln289, and the Glut5-specific Asn294 – residues also found to be involved in fructose uptake through GLUT5 [23]. While the binding of 1-AM between three complexes involved the same residues, the H-bonding sites at 1-AM were altered to accommodate the change in the position of the fluorophore. For ManCou1, the large population of conformers was found to orient the coumarin moiety towards His419 and Trp420 – residues found to be critical for fructose uptake (Figure 2.3A) [23]. For

ManCou3, nine out of ten conformational isomers had the coumarin moiety oriented away from these residues into the more open space (Figure 2.3C). Interestingly, for ManCou2 (Figure 2.3B), conformations similar to those of ManCou1 and ManCou3 were detected, suggesting the probe to have duality, as sensed by malignant cells. However, a higher level modeling would be required to assess a true binding site(s) for these probes and further identifying key interactions contributing to the differences in their uptake behavior and cellular impact.

2.4 Analysis of ManCou1-3 uptake

The uptake analysis of ManCou1-3 was carried out in breast cancer (adenocarcinoma) MCF7 cells. MCF7 cells have been previously studies for GLUT5-mediated uptake [15, 24-26] thus providing a good platform for initial probe evaluation. MCF7 cells were cultured according to standard protocol, seeded in the 96-well plate (20000 cells/well) and maintained to adhere for 12 h. Cells were then treated with varied concentrations of ManCous 1-3 (in Hank's solution and media) for 10 min at 37 °C, and fluorescence was measured after removal of the probe and cell wash. As a result, efficient concentration-dependent uptake was observed for all probes with ManCou1 having the highest uptake and ManCou3 having the lowest uptake (Figure 2.4A). The transported probe remains in the cells even after post-incubation in a probe-free media and repeated washing. This is in agreement with previous observations, where 2,5-anhydro-D-mannitol was found to be a suitable substrate for phosphofructokinase-1 [27-29]. Accordingly, the lack of back transport is a significant point because GLUT transporters, being antiporters, take up and excrete

carbohydrates, but not the phosphorylated products [30]. The comparative analysis of non-conjugates coumarins with ManCou (Figure 2.4B) shows that the presence of 1-AM drastically enhances the uptake, putatively contributing to facilitative internalization of probes rather than passive diffusion (as for non-conjugated coumarins).

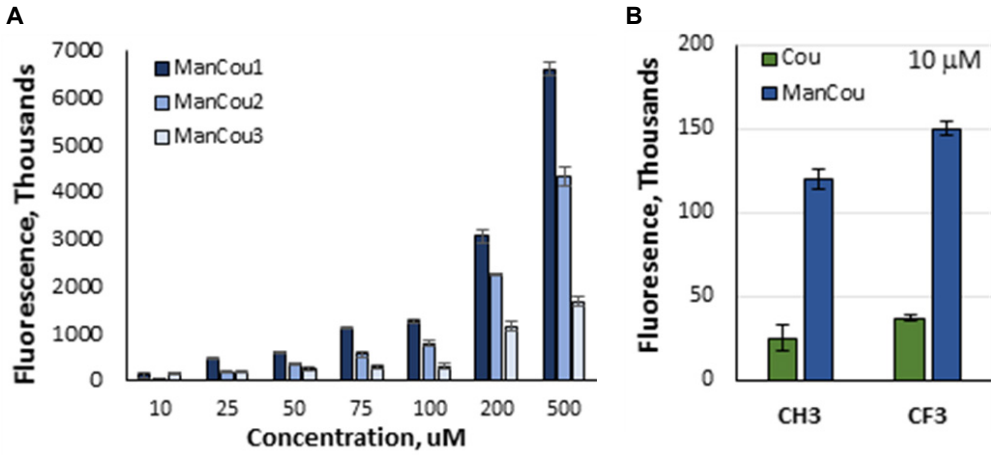

Figure 2.4. Uptake analysis of ManCou probes in MCF7 cells. A) ManCou probes exhibit concentration-dependent uptake. B) 1-AM facilitates coumarin uptake (measured for 20 µM ManCou1-3 vs. non-conjugates coumarins). Data represents the Gained Fluorescence (excitation at 385 nm) measured in a 96-well plate settings after 10 min incubation of cells with probes in Hank's buffer. Fluorescence values corrected for the quantum yield of ManCou probes.

24 hours after the uptake no ManCou-induced fluorescence activity was observed, suggesting cellular metabolism of the fluorophore. This observation, as well as no saturated fluorescence point being found, points toward ManCou sugar base undergoing phosphorylation as it enters the cell to and eventually being excreted as a metabolite. If the sugar base was not phosphorylated, the probe could easily be excreted once the media containing the fluorophore was removed, which was not

observed even after 30min post incubation. Further testing is needed to determine whether the fluorophore itself is metabolized or passively diffuses out of the cell.

The uptake efficiency of ManCou probes appears to change with the change in electronic properties of coumarins. Thus, from three probes, ManCou1 is taken up most avidly, ManCou2 is taken up with ~25%, and ManCou3 with 4-fold lesser efficiency (Figure 2.4A). The analysis of the uptake kinetics through Michaelis-Menten method [18] showed all three probes to have concentration-dependent saturable uptake (Figure 2.5), exceeding that of fructose by nearly 1000-fold (15-17 μM for ManCou1 and 2, and 35-37 μM for ManCou3).

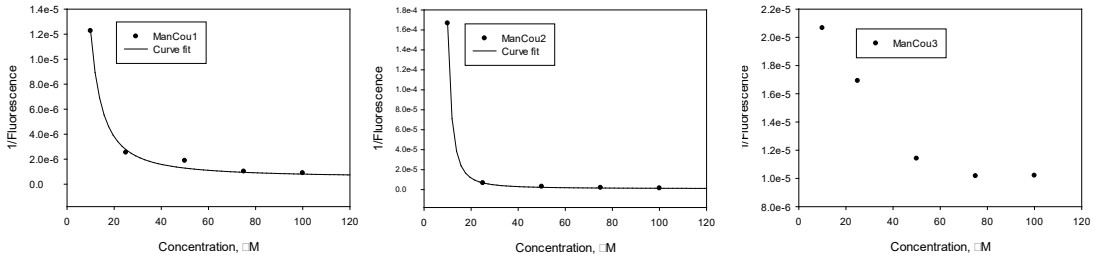

Figure 2.5. Kinetic analysis of ManCou1-3 uptake using Michaelis-Menten Kinetics. Plots depict 1/fluorescence vs. 1/concentration using data obtained upon treating cells with 1-100 μM ManCou concentrations Plots obtained with SigmaPlot13.

The Z-stack images obtained for MCF7 cells treated with ManCous 1-3 show that while ManCou1 and 2 are localized within the membrane and in the cytosol, ManCou3 is only present within the cell membrane. The drastic difference in probe properties could be rising due to the extended binding of ManCou3 with GLUT5, and particularly with Trp419. From all residues identified to bind ManCou3, the Trp419 is a key residue located on the transmembrane helix 11 (TM11) of GLUT5 which may inhibit the conformation shift between TM10 and TM7 required for the change from the

occluded state into the inward open state. In such case, the protein is expected to be locked in the outward-open conformation and prevent internalization of the substrate. However, it would require a crystal structure with probe bound to confirm this notion.

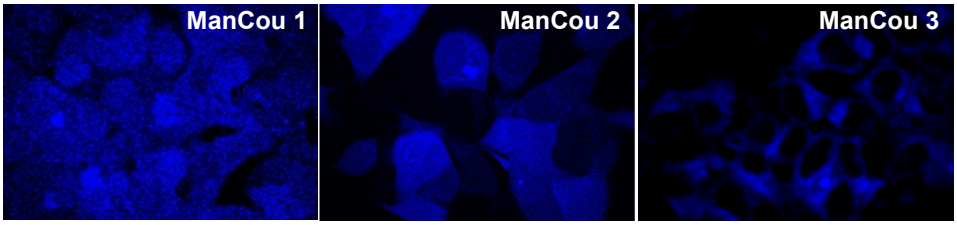

Figure 2.6. Confocal Z-stack images of MCF7 cells treated with 20 uM ManCou1-3 (10 min at 37 °C, 405 nm excitation, 461 nm (DAPI) emission, 60X objective).

To assess whether ManCou1-3 exhibit GLUT5 specificity, the impact of nutrient carbohydrates, MNBD, GNBD, and cytochalasin B on the probe uptake was evaluated. Glucose, fructose, and glucosamine were used as competitive inhibitors of ManCou uptake. The impact of glucose and fructose on the uptake was used to establish the involvement of glucose transport and fructose transport, respectively, in the ManCou uptake. Upon addition of glucose up to concentrations exceeding physiological (1-50 mM) no inhibition of ManCou uptake was detected (Figure 2.7A). Likewise, no significant change in the uptake efficiency of ManCou probes was observed upon crying out uptake analysis in culture media, as opposed to Hank's buffer (Figure 2.7B). These results could rise from the significantly higher affinity of ManCou probes to their biological target(s), resulting in a lack of interference of nutrients in their uptake. ManCou uptake is however inhibited by MNBD, previously shown to target GLUT5, while not impacted by GNBD (targeting glucose transport).

The observation is suggestive of ManCou probes exhibiting the same mechanism of uptake as MNBD, i.e. via GLUT5.

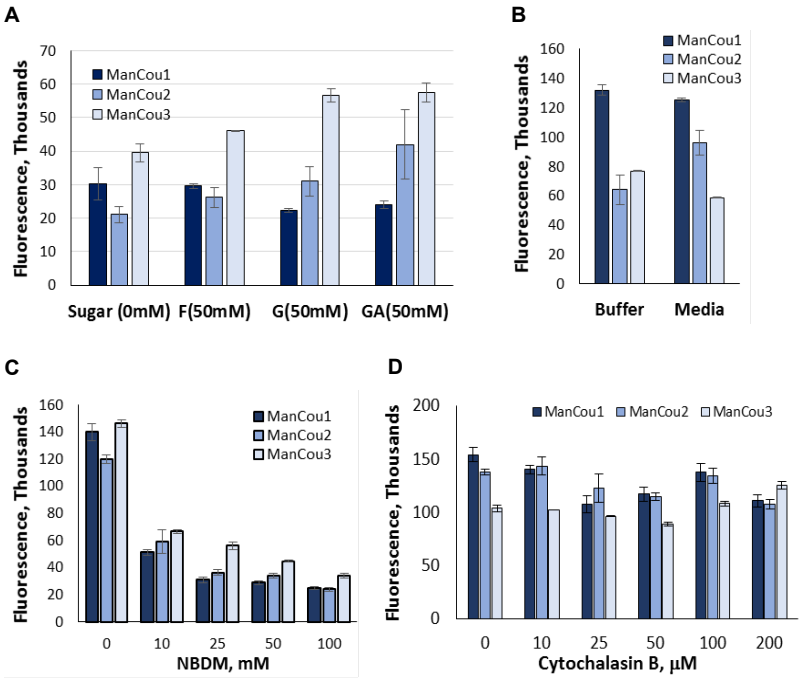

Figure 2.7. Inhibition of ManCou (20 µM) uptake with carbohydrates (A), culture media (B), MNDB (C), GNDB (D), and cytochalasin B (E) in MCF7 cells. Data normalized by quantum yield.

To further assess the role other fructose transporters in ManCou uptake - particularly the role of GLUT2 contributing ~12% to total fructose uptake in MCF7 cells - cytochalasin B was used a non-competitive inhibitor of glucose uptake through GLUTs 1-4. Addition of cytochalasin B in concentrations far exceeding the established for GLUTs 1-4 (K_i = 2-10 µM) did not have impact on the uptake of ManCou probes, showing the uptake to be independent of GLUT1-4. The use of glucosamine (up to 50 mM) as GLUT2-specific substrate also did not induce any effect on ManCou uptake, further supporting the lack of GLUT2 participation in the uptake of ManCou probes.

Overall, uptake inhibition studies strongly suggest that ManCou probes are transported through fructose-specific transporter GLUT5.

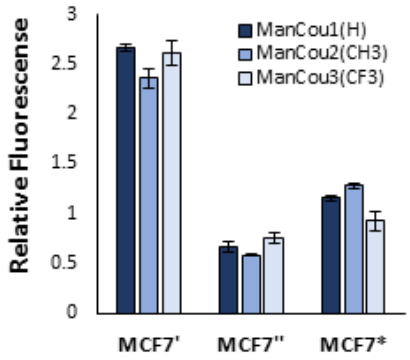

Figure 2.8: Uptake of ManCous in MCF7 cells pre-conditioned with or without fructose. Comparative analysis of ManCou uptake in fructose-fed (MCF7'), fructose-deprived (MCF7") and fructose re-fed (MCF7*) cells (normalized by MCF7). MCF7, cells grown in standard media; MCF7', cells fed with fructose; MCF7", cells deprived of fructose; MCF7*, MCF7" cells re-fed with fructose. Data represents the Gained Fluorescence. Fluorescence values corrected for the quantum yield of ManCou probes.

Prolonged exposure of cells to fructose has been shown to primarily increase expression of GLUT5 [31]. Hence, preconditioning of MCF7 cells with fructose has been carried out to gather further evidence of GLUT5-mediated uptake of ManCou1-3. To produce fructose-fed cells, MCF7 cells were maintained in the standard growth media supplemented with 11mM fructose for ten days. The uptake analysis of ManCu1-3 probes in fructose-fed MCF7' cells showed up to 3-fold increase in uptake of ManCou probes (Figure 6A). These results are consistent with previously reported MNBD uptake with fructose preconditioned MCF7 cells [16]point towards GLUT5 driven uptake of ManCou as a result of increased activity of fructose transport or metabolism. Starving MCF7 cells of fructose by maintaining them in the dialyzed media for ten days decreased ManCou uptake by 2-fold while re-feeding the starved cells by

maintaining them in regular media (non-dialyzed) regenerated the levels of the uptake. Whether the observed changes result from the alterations in GLUT5 expression or are driven by the changes in metabolic activity of preconditioned cells has not yet been determined.

Overall, the inhibition and cell preconditioning studies indicate that Manzcou1-3 probes are preferentially transported through GLUT5. Within this set of probes, ManCou1 behaves as a transport probe, showing clean gradient-driven uptake kinetics of first-order in the ManCou. ManCou3 appears to be an effective transport-labeling probe showing clean receptor-ligand kinetics. ManCou2, overall, shows behavior is similar to ManCou1 (i.e. is transported through the membrane). However, some interactions with the protein appear to deviate the uptake from pure gradient driven first order kinetics.

2.5 ManCous as GLUT5 expression and fructose metabolism probes

To further determine ManCou's method of transport, several different human cancerous and noncancerous cell lines known to have different expression of GLUT5 were treated with ManCou 1-3 probes. In normal breast MCF10A cells, known to have minimal levels of GLUT5 expression, ManCous have shown significantly lesser uptake compared to the cancerous counterparts. This is expected due to documented increase in carbohydrate uptake in cancerous cells when compared to their noncancerous equivalents. Interestingly H9C2 a cardiac cell line showed minimal to no uptake of ManCou1 or 2. However, labeling of the membrane with ManCou3 showed results similar to that of MCF7 cells. While the expression levels of GLUT5 in

H9C2 are not established, it appears that the differences in fluorescence induction by ManCou1 vs. Mancou3 may be indicative of a sufficient membrane expression of GLUT5 but the lack of metabolizing enzymes to drive gradient-dependent transport of ManCou1. This observation provides grounds for further analysis of protein (GLUT5 vs. metabolizing kinases) expression in cardiac cells. Subsequently, ManCou probes could be effectively used to identify GLUT5 expression and fructose metabolism in cells.

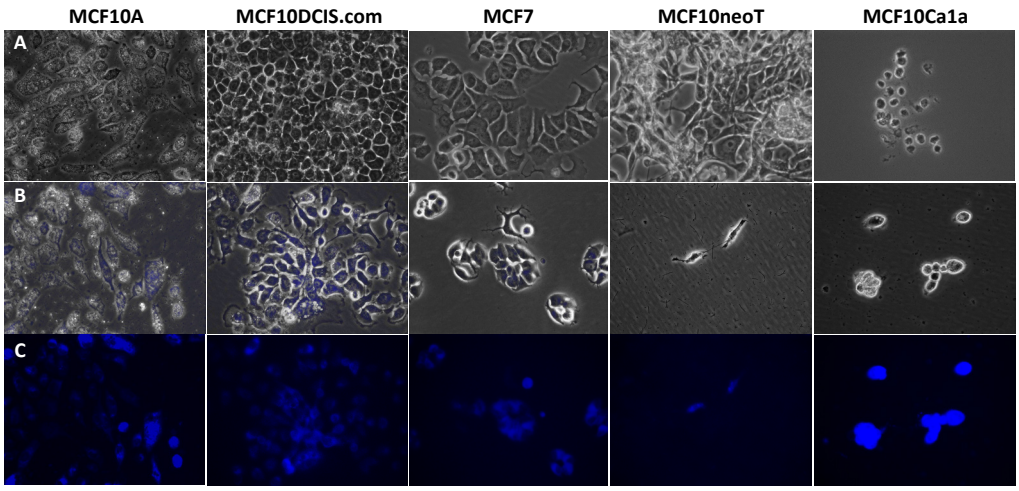

Figure 2.9. ManCous1 and ManCou3 in the MCF10A model (confocal images): A) cells with no probe; B) cells with the probe; C) cells with the probe (fluorescence). MCF10A, non-cancer; MCF10DCIS.com, undifferentiated lesions, MCF7, adenocarcinoma; MCF10-neoT, premalignant; and MCF10Ca1a, highly malignant. Images taken at 405 nm laser at 461 nm (DAPI) emission (20X objective).

Considering that there is currently a significant lack in understanding what impact fructose uptake inhibition may have on cells, we have evaluated ManCou3 in a MCF10 model that systemically demonstrate breast cancer initiation, development, and progression [32]. As a result, blocking Glut5 with ManCou3 exerted cytotoxic response in malignant cells but not in normal or undifferentiated cells (Figure 2.9).

2.6 Conclusions

Here three novel carbohydrate-mediated probes have been developed and tested, each with their unique kinetics of intercellular uptake. ManCou1 and 2 both appear to pass through GLUT5, ManCou3 appears to remain inside the cellular membrane. Considering the link between GLUT5 activity and carcinogenesis [33] targeting GLUT5 appears to give a new way to achieve cancer-specificity of therapeutics or imaging agents. In fact, ManCou probes appears to exhibit desired cancer specificity. Moreover, blocking Glut5 with ManCou3 exerted cytotoxic response in malignant cells but not in normal or undifferentiated cells. These results may potentially lead to a procedure for relatively quick analysis on cancer aggressiveness based on fluorescent intensity and accumulation. Also, ManCous provide a proof of concept that using carbohydrate mimics, such as 1-AM, may be beneficial for targeted drug delivery.

References:

1. Marger, M.D. and M.H. Saier, Jr., *A major superfamily of transmembrane facilitators that catalyse uniport, symport and antiport.* Trends Biochem. Sci., 1993. **18**(1): p. 13-20.
2. Manolescu, A.R., et al., *Facilitated hexose transporters: new perspectives on form and function.* Physiology, 2007. **22**: p. 234-40.
3. Brockmann, K., *The expanding phenotype of GLUT1-deficiency syndrome.* Brain Dev., 2009. **31**(7): p. 545-552.
4. Adekola, K., S.T. Rosen, and M. Shanmugam, *Glucose transporters in cancer metabolism.* Curr. Opin. Oncol., 2012. **24**(6): p. 650-654.
5. McQuade, D.T., M.B. Plutschack, and P.H. Seeberger, *Passive fructose transporters in disease: a molecular overview of their structural specificity.* Org. Biomol. Chem., 2013. **11**(30): p. 4909-4920.
6. Stein, W.D., *The mechanism of sugar transfer across erythrocyte membranes.* Ann. N.Y. Acad. Sci., 1972. **195**: p. 412-28.
7. Barnett, J.E., G.D. Holman, and K.A. Munday, *Structural requirements for binding to the sugar-transport system of the human erythrocyte.* Biochem. J., 1973. **131**(2): p. 211-221.
8. Colville, C.A., M.J. Seatter, and G.W. Gould, *Analysis of the Structural Requirements of Sugar Binding to the Liver, Brain and Insulin-Responsive Glucose Transporters Expressed in Oocytes.* Biochem. J., 1993. **294**: p. 753-760.

9. Colville, C.A., et al., *Kinetic-Analysis of the Liver-Type (Glut2) and Brain-Type (Glut3) Glucose Transporters in Xenopus Oocytes - Substrate Specificities and Effects of Transport Inhibitors.* Biochem. J., 1993. **290**: p. 701-706.
10. Nishimura, H., et al., *Kinetics of Glut1 and Glut4 Glucose Transporters Expressed in Xenopus Oocytes.* J. Biol. Chem., 1993. **268**(12): p. 8514-8520.
11. Tatibouet, A., et al., *Synthesis and evaluation of fructose analogues as inhibitors of the D-fructose transporter GLUT5.* Bioorgan. Med. Chem., 2000. **8**(7): p. 1825-1833.
12. Calvaresi, E.C. and P.J. Hergenrother, *Glucose conjugation for the specific targeting and treatment of cancer.* Chem. Sci., 2013. **4**(6): p. 2319-2333.
13. Chen, Q., et al., *Synthesis, in vitro and in vivo characterization of glycosyl derivatives of ibuprofen as novel prodrugs for brain drug delivery.* J. Drug Target., 2009. **17**(4): p. 318-328.
14. Zou, C.H., Y.J. Wang, and Z.F. Shen, *2-NBDG as a fluorescent indicator for direct glucose uptake measurement.* J. Biochem. Biophys. Meth., 2005. **64**(3): p. 207-215.
15. Levi, J., et al., *Fluorescent fructose derivatives for imaging breast cancer cells.* Bioconjugate Chem., 2007. **18**(3): p. 628-634.
16. Tanasova, M., et al., *Fluorescent THF-Based Fructose Analogue Exhibits Fructose-Dependent Uptake.* ChemBioChem, 2013. **14**(10): p. 1263-1270.
17. Douard, V. and R.P. Ferraris, *Regulation of the fructose transporter GLUT5 in health and disease.* Am J Physiol Endocrinol Metab, 2008. **295**(2): p. E227-37.

18. Gigantesco, A., et al., *[Depressive symptoms, a challenge for the community of L'Aquila after the earthquake of 2009].* Epidemiol Prev, 2012. **36**(2): p. 129.
19. Tatko, C.D. and M.L. Waters, *Effect of halogenation on edge-face aromatic interactions in a beta-hairpin peptide: Enhanced affinity with Iodo-substituents.* Organic Letters, 2004. **6**(22): p. 3969-3972.
20. Rahman, A.N.M.M., et al., *Pi-halogen dimer interactions and the inclusion chemistry of a new tetrahalo aryl host.* Org. Biomol. Chem., 2004. **2**(2): p. 175-182.
21. Plutschack, M.B., et al., *Flow synthesis of a versatile fructosamine mimic and quenching studies of a fructose transport probe.* Beilstein J. Org. Chem., 2013. **9**: p. 2022-7.
22. Melhuish, W.H., *Quantum Efficiencies of Fluorescence of Organic Substrates: Effect of Solvent and Concentration of the Fluorescent Solute.* J. Phys. Chem., `1961. **65**(2): p. 229–235.
23. Nomura, N., et al., *Structure and mechanism of the mammalian fructose transporter GLUT5.* Nature, 2015. **526**(7573): p. 397-401.
24. Zamora-Leon, S.P., et al., *Expression of the fructose transporter GLUT5 in human breast cancer* Proc. Nat. Acad. Sci. U.S.A., 1996. **93**(26): p. 15522-15522.
25. Zamora-Leon, S.P., et al., *Expression of the fructose transporter GLUT5 in human breast cancer.* Proc. Natl. Acad. Sci. U.S.A., 1996. **93**(5): p. 1847-1852.
26. Gowrishankar, G., et al., *GLUT 5 Is Not Over-Expressed in Breast Cancer Cells and Patient Breast Cancer Tissues.* PLoS ONE, 2011. **11**: p. e26902-e26909.

27. Koerner, T.A., Jr., et al., *The fructose 6-phosphate site of phosphofructokinase. I. Tautomeric and anomeric specificity.* J. Biol. Chem., 1974. **249**(18): p. 5749-5754.
28. Raushel, F.M. and W.W. Cleland, *The substrate and anomeric specificity of fructokinase.* J. Biol. Chem., 1973. **248**(23): p. 8174-8177.
29. Dills, W.L., et al., *2,5-Anhydro-1-Deoxy-D-Lyxitol, 2,5-Anhydro-1-Deoxy-D-Mannitol, and 2,5-Anhydro-1-Deoxy-D-Talitol - Synthesis and Enzymic Studies.* Carbohyd. Res., 1982. **99**(1): p. 23-31.
30. Azema, L., et al., *Interaction of substituted hexose analogues with the Trypanosoma brucei hexose transporter.* Biochem. Pharmacol., 2004. **67**(3): p. 459-467.
31. Mesonero, J., et al., *Sugar-dependent expression of the fructose transporter GLUT5 in Caco-2 cells.* Biochem J, 1995. **312 (Pt 3)**: p. 757-62.
32. Rhee, D.K., S.H. Park, and Y.K. Jang, *Molecular signatures associated with transformation and progression to breast cancer in the isogenic MCF10 model.* Genomics, 2008. **92**(6): p. 419-428.
33. Godoy, A., et al., *Differential subcellular distribution of glucose transporters GLUT1-6 and GLUT9 in human cancer: Ultrastructural localization of GLUT1 and GLUT5 in breast tumor tissues.* J. Cel. Physiol., 2006. **207**(3): p. 614-627.

Chapter 3

Synthesis of Locked Fructose Analogs

3.1 Introduction

MNBD (1-amino-2,5-deoxy-D-mannitol conjugated to NBD) has been shown to preferentially transported through GLUT5 with significantly higher affinity for fructose. However, it is unclear what exactly leads to the observed increased affinity. One of the possibilities is that GLUT5 may have a preference for the five-member ring conformation in addition to hydrophobic interactions induced by the fluorophore. Fructose equilibrates between two different ring conformations; furanose (five-membered ring) and pyranose (six-membered ring) with 25% and 75% populations respectfully. GLUT5 affinity towards these ring conformations are unclear due to all probes used to determine it exist as anomeric mixtures [1, 2]. To alleviate these ambiguous results, probes need to be developed with locked ring conformations to understand if GLUT5 is specific for pyranose or furanose forms of the sugar.

Fructose has four stereocenters. However, the importance of their absolute stereochemistry is unclear. Altering these stereocenters may lead to increased binding affinity towards the transporter which may lead to potentially potent inhibitors. Using organic synthetic techniques to install each stereocenter will allow the construction of several unique probes to determine importance of stereochemistry on GLUT5 uptake. This chapter outlines the goals and current progress of probe synthesis.

3.2 Results and Discussion

While synthetic development proceeded smoothly for initial reactions in relatively high yields, the first significant challenge in the synthesis was the apparently simple oxidation of the epoxy system. Common oxidation techniques such as PCC and Swern yielded little to no results, however when **1** was subjugated to Parikh-Doering conditions the resulting aldehyde was obtained in relatively high yield. Wittig olefination proceeded smoothly followed by *syn*-selective opening using Pd tetrakis in the presence of benzyl alcohol. Followed by DIBAL reduction which lead to relatively high yield of 83%. After the isolation of **3** the initial goal was to oxidize the epoxy alcohol, extend and repeat the Pd-catalyzed opening. However, TEMPO oxidation techniques to selectively oxidize the primary alcohol did not proceed. Parekh-Doering was then conducted to attempt to get the aldehyde but ultimately proved unsuccessful.

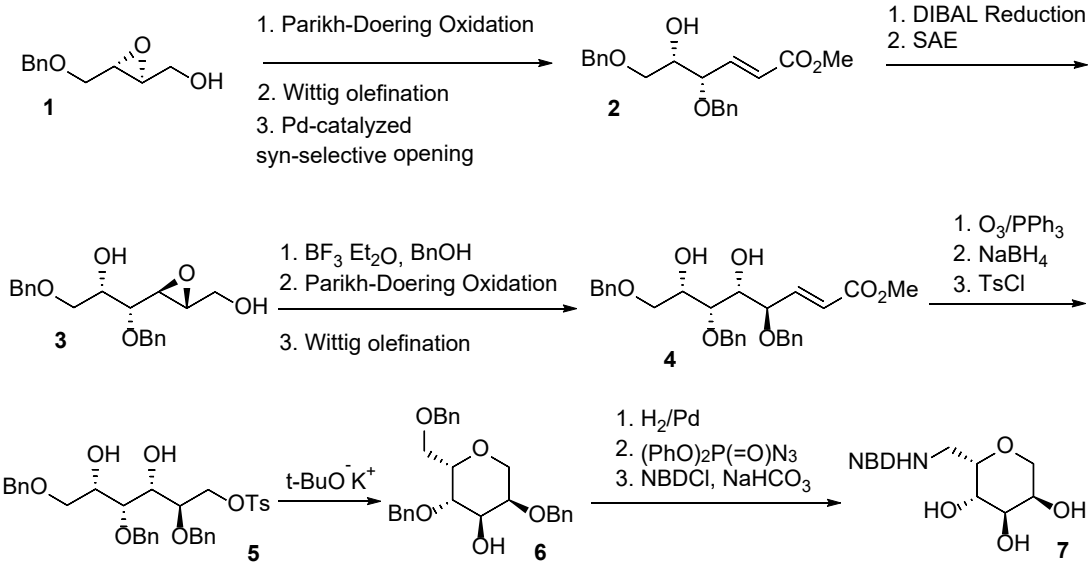

Scheme 3.1: Overall synthesis of alpha-NBD pyranose probe

Moving forward the synthesis will be altered on opening the second epoxide using a more traditional *anti*-opening using a Lewis acid and nucleophile. Following reactions are expected to yield similar results to previous attempts before arriving at **4.** Ozonolysis should proceed smoothly to cleave double bond and sequential carbonyl reduction using $NaBH_4$ to generate a primary alcohol. Primary alcohol will be tosylated using Tosyl chloride (TsCl) before undergoing intercellular cyclization. After generation of locked pyranose, the synthetic steps can be easily modified to generate altering stereochemistry through Sharpless asymmetric epoxidation to test the effect of altering stereocenters.

This synthesis can be easily altered to generate furanose locked analogs by simply stopping after secondary SAE and cyclizing. This will be explored in the future as both furanose and pyranose probes are developed to further understand the importance of sugar ring size in fructose transport.

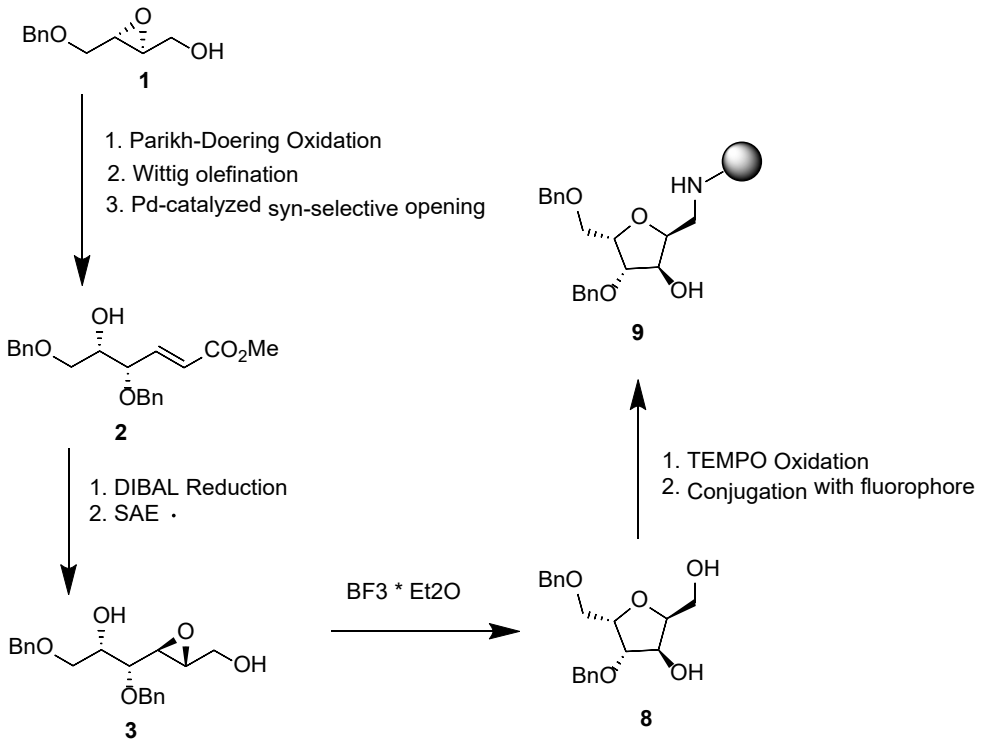

Scheme 3.2: Synthesis of locked furanose probe

3.3 Conclusions

Initial groundwork has been developed for a series of probes designed to effectively determine stereocenter and ring size importance in fructose transport. With synthetic optimizations, these probes should be able to be made on milligram scale and carried over for cellular studies.

3.4 Experimental

All reactions (unless otherwise stated) were done with flame dried glassware and using commercially available reagents without further purification from Sigma-Aldrich. Silica gel was purchased from Siliflash and has a size of 43-63 μm. Solvents

used were taken from dried source. Column chromatography was performed using SiliCycle silica gel (230-400 mesh). Thin layer chromatography (TLC) was performed using Sigma-Aldrich TLC plates over aluminum support 200um thickness with 25 μm particle size. Structural analysis of compounds was carried out with 400 MHz Varian NMR instrument. Spectra are reported in parts per million (ppm) relative to the solvent resonances (δ), with coupling constants (*J*) in Hertz (Hz).

Benzyl Protection of alkyne

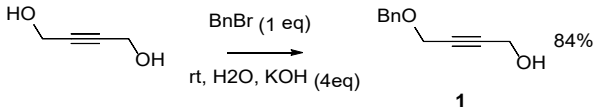

1

1,4-butynediol (20 g, 232 mmol, 4 eq) was dissolved in 200 mL of deionized water at room temperature and allowed to stir until dissolved. After starting material was dissolved potassium hydroxide (13 g, 232 mmol, 4 eq) was added and allowed to stand for 30 min. After 30min benzyl bromide was added dropwise and allowed to stir overnight. Solution was then extracted with 3 treatments of 75 mL of diethyl ether and dried over sodium sulfate. Solvent was removed under reduced pressure to leave the yellow crude oil (9.2g) and was then purified over silica gel using ethyl acetate/hexane (10/90)solvent system to yield **1** in 84% yield[3]. ^{1}H-NMR $CDCl_3$: δ 7.2 (m, 5H), 4.80 (s, 2H), 3.80 (d, 2H), 3.90 (d, 2H), 2.8 (s, b, 1H).

Reduction of alkyne to *trans*-alkene.

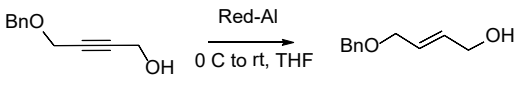

Alkyne **1** (9 g, 50.3 mmol) dissolved in 100 mL of dry THF and cooled to 0 C° under Ar atmosphere. Red-Al (60% toluene, 30 g, 87 mmol) was then added dropwise over a course of 10 min via syringe. Reaction allowed to stand for 1 hour at room temperature. Reaction was cooled to 0 C° and 100 mL of 10% sulfuric acid was added to quench reaction. The resulting biphasic system was extracted with three times with 75 mL of dichloromethane. Solvent was removed under reduced pressure to give very light yellow oil (7.8 g) and then purified over silica gel using ethyl acetate/hexane (10/90) solvent system to yield **2** in 72% yield [4]. ^{1}H-NMR $CDCl_3$: δ 7.1 (m, 5H), 5.9 (m, 2H), 4.7 (s, 2H), 4.1 (d, 2H), 4.0 (d, 2H), 2.8 (b, 1H)

Sharpless asymmetric epoxidation (SAE)

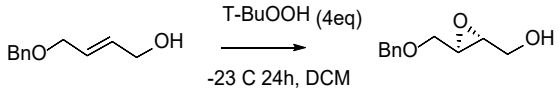

Dried molecular sieves 4Å (4.0 g) were added to dry dichloromethane in a flame dried flask at -23 C° before both titanium tetra(isopropoxide) (0.25 eq) and (-) diethyl tartrate (0.36 eq) are added to solvent under Ar atmosphere. Dried *tert*-butyl hydroperoxide 3.5M solution in toluene (4eq) was added dropwise over 20min before allowing solution to stand with stirring for 30 min. After allotted time allylic alcohol (1 eq) was dissolved in of dried dichloromethane and added to solution dropwise over 1hr. Reaction was kept at -20 C° overnight before being warmed to room temperature and quenched with 30% NaOH solution in water and stirred for 20 min. The molecular sieves were, and salts were then filtered off using vacuum filtration before the two phases were separated. Aqueous phase was extracted with three washes of 75 mL of dichloromethane. Resulting organic phase was dried over

sodium sulfate and concentrated under reduced pressure, followed by purification using column chromatograph (silica gel, 10/90 EtOAc-hexane). Resulting in epoxide in 78% yield [5]. ^{1}H-NMR $CDCl_3$: δ 7.2 (m, 5H), 4.6 (dd, 2H), 3.9 (m, 1H), 3.7 (dd, 1H), 3.5 (m, 1H), 3.4 (dd, 1H), 3.2 (m, 1H), 2.9 (b, 1H)

Parikh-Doering oxidation of 3

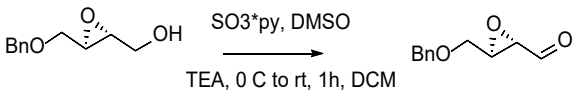

To a dried flask dichloromethane (4.3 mL/mmol) and dimethylsulfoxide (0.73 mL/mmol) were cooled to 0 C° before epoxy alcohol was added to solution with stirring under Ar atmosphere. To this solution, TEA (3 eq) was added via syringe, and sulfur trioxide pyridine complex (4 eq) purchased from TCI was added rapidly. Solution turns from clear to a light brown/red and is allowed to come to room temperature. After 2 h, reaction was monitored by TLC before being cooled back down to 0 C°. Reaction is quenched by a saturated solution of copper sulfate pentahydrate and extracted with dichloromethane. Organic phase was dried over sodium sulfate and concentrated under reduced pressure before being purified by column chromatography (silica gel, 30/70 EtOAc-hexane). Aldehyde was purified to give 53% yield [6]. ^{1}H-NMR $CDCl_3$: δ 10.4 (d, 1H), 7.2 (m, 5H), 4.6 (dd, 2H), 3.9 (m, 1H), 3.7 (dd, 1H), 3.5 (m, 1H), 3.4 (dd, 1H), 3.2 (m, 1H)

3.5 Additional Information

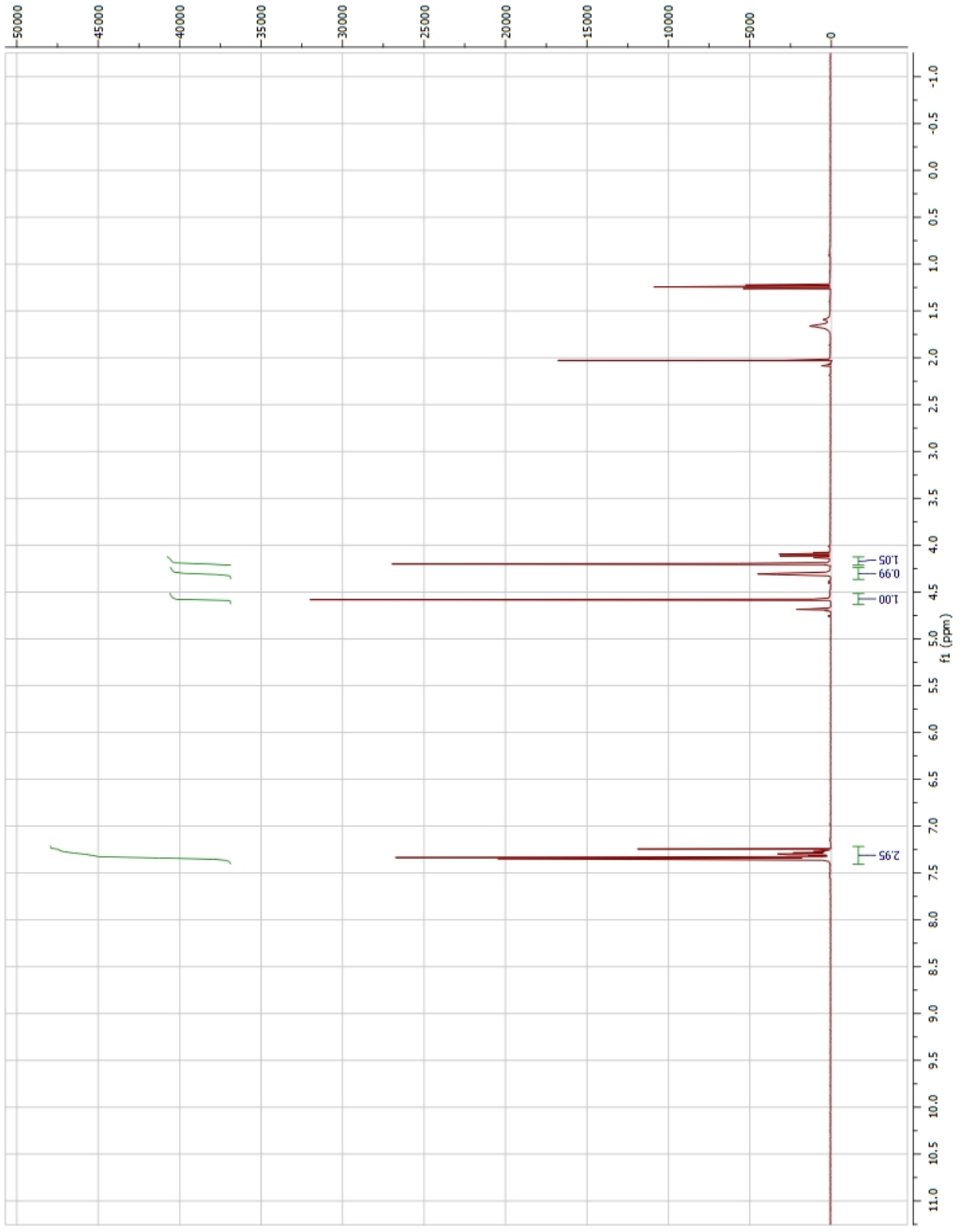

Figure 3.1 H^1 NMR at 400Hz for 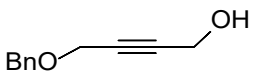

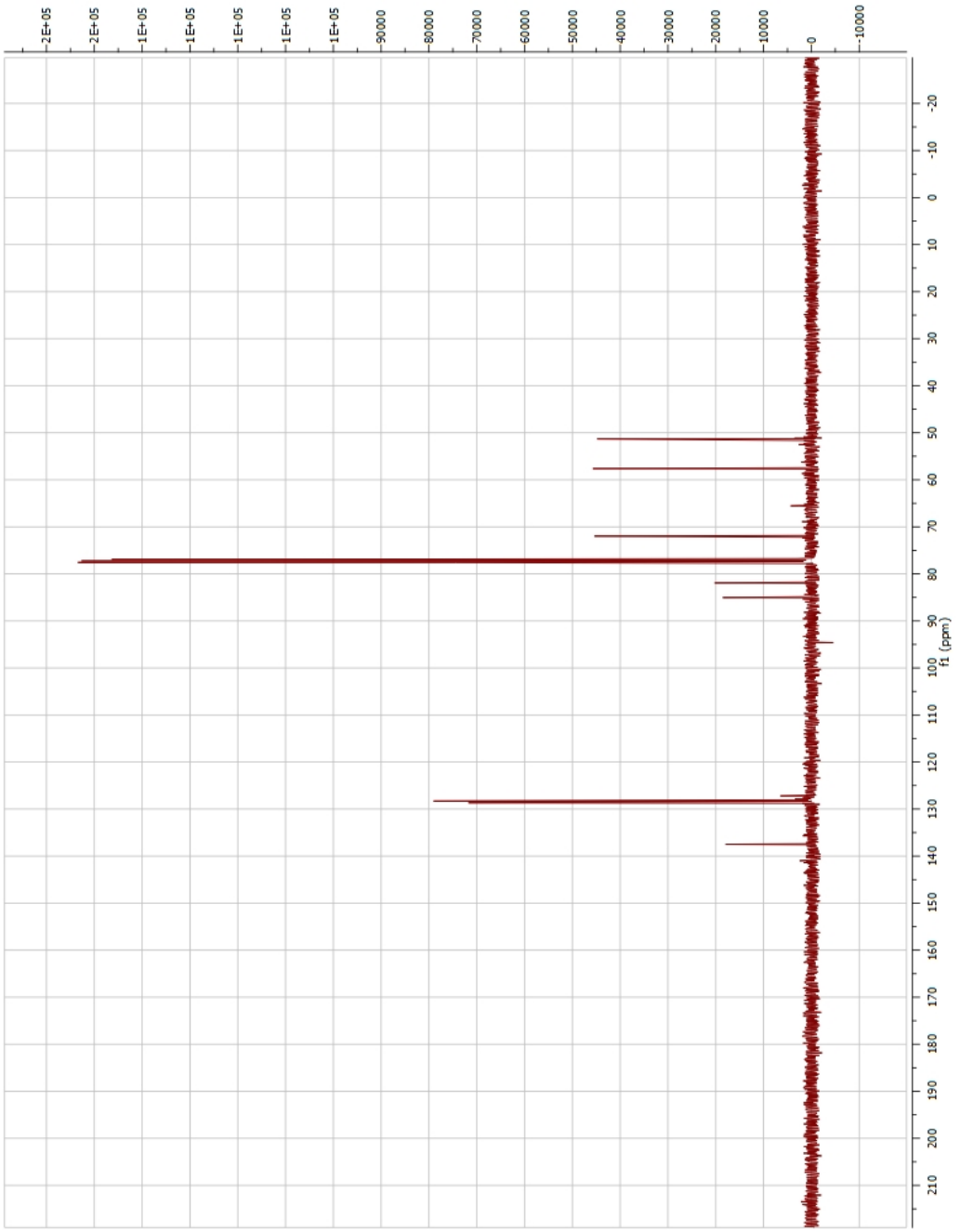

Figure 3.2 C^{13} NMR at 400Hz for 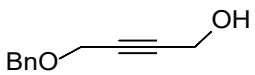

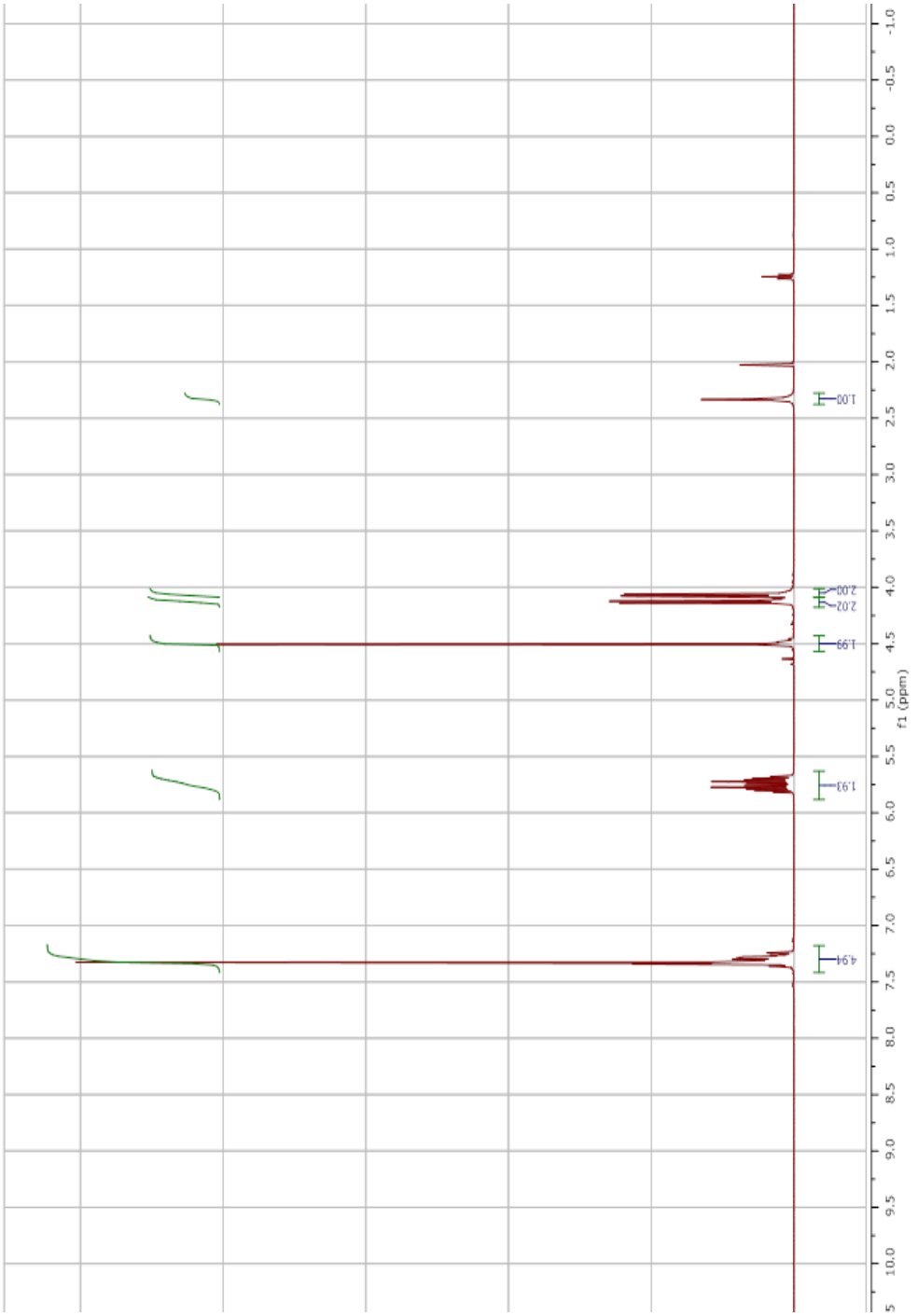

Figure 3.3 H^1 NMR at 400 Hz for 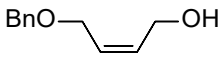

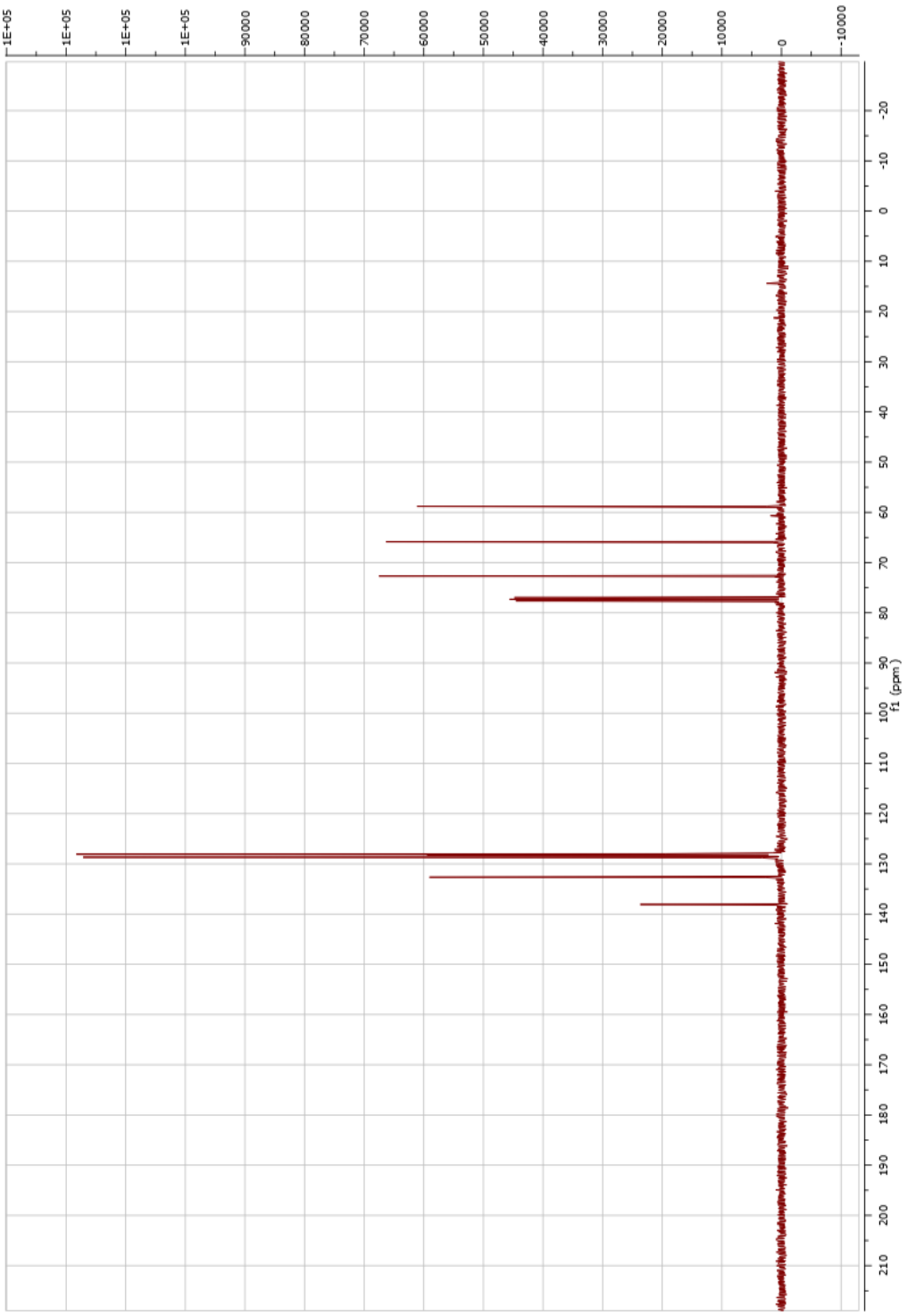

Figure 3.4: C^{13} at 400Hz for 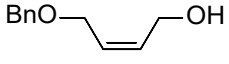

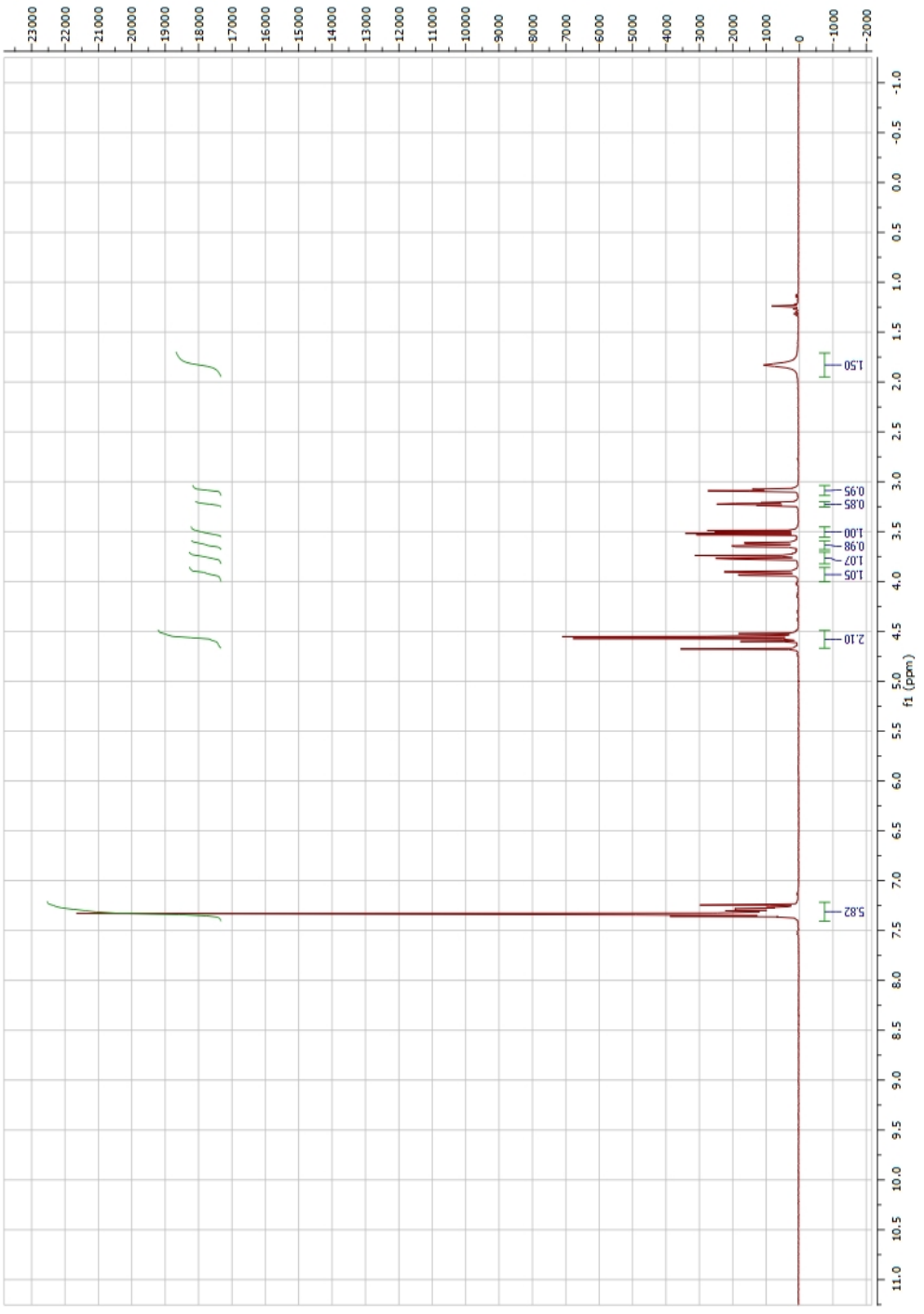

Figure 3.5: H^1 NMR at 400Hz for 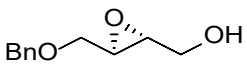

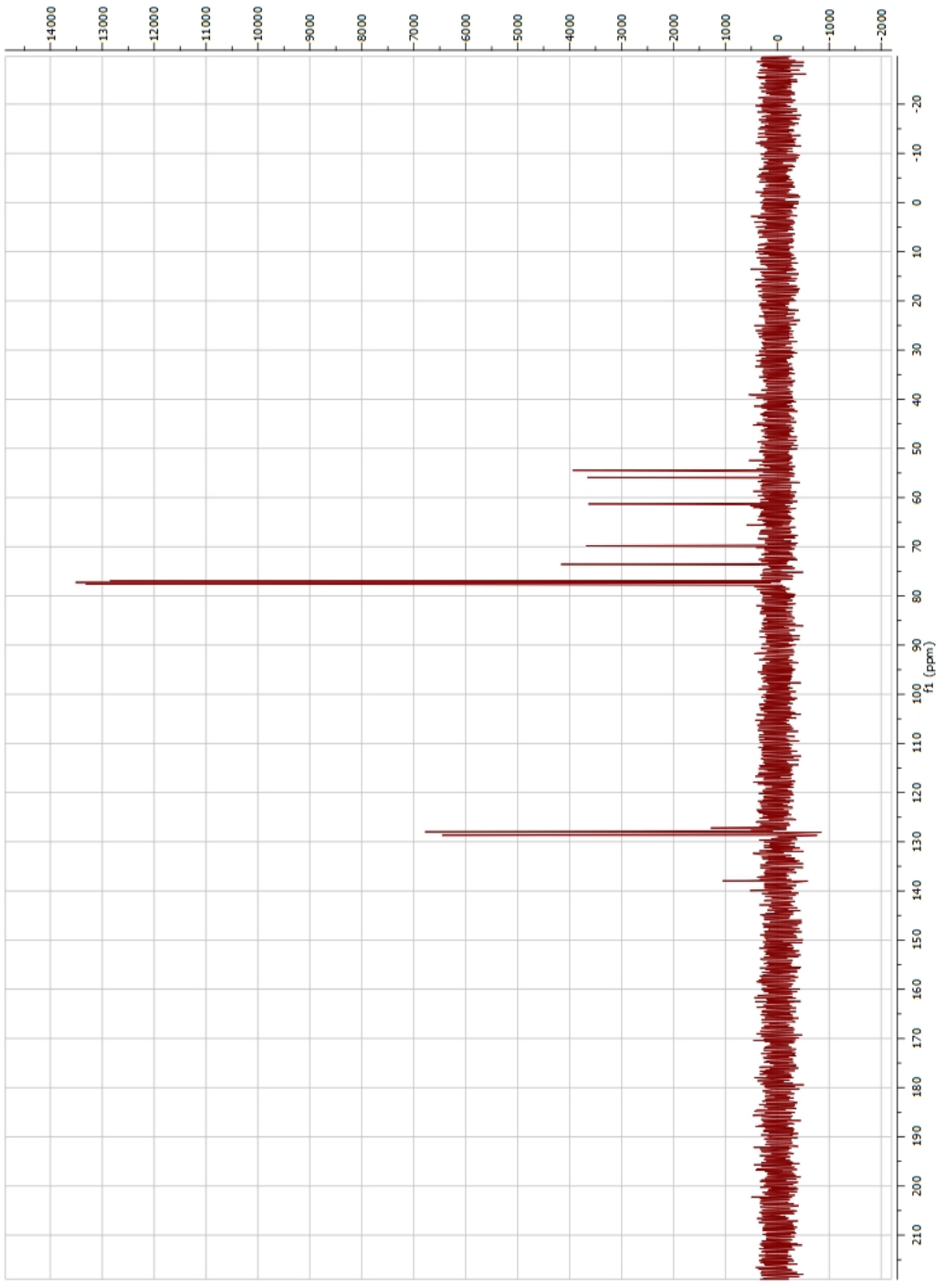

Figure 3.6 C^{13} at 400Hz for 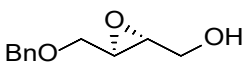

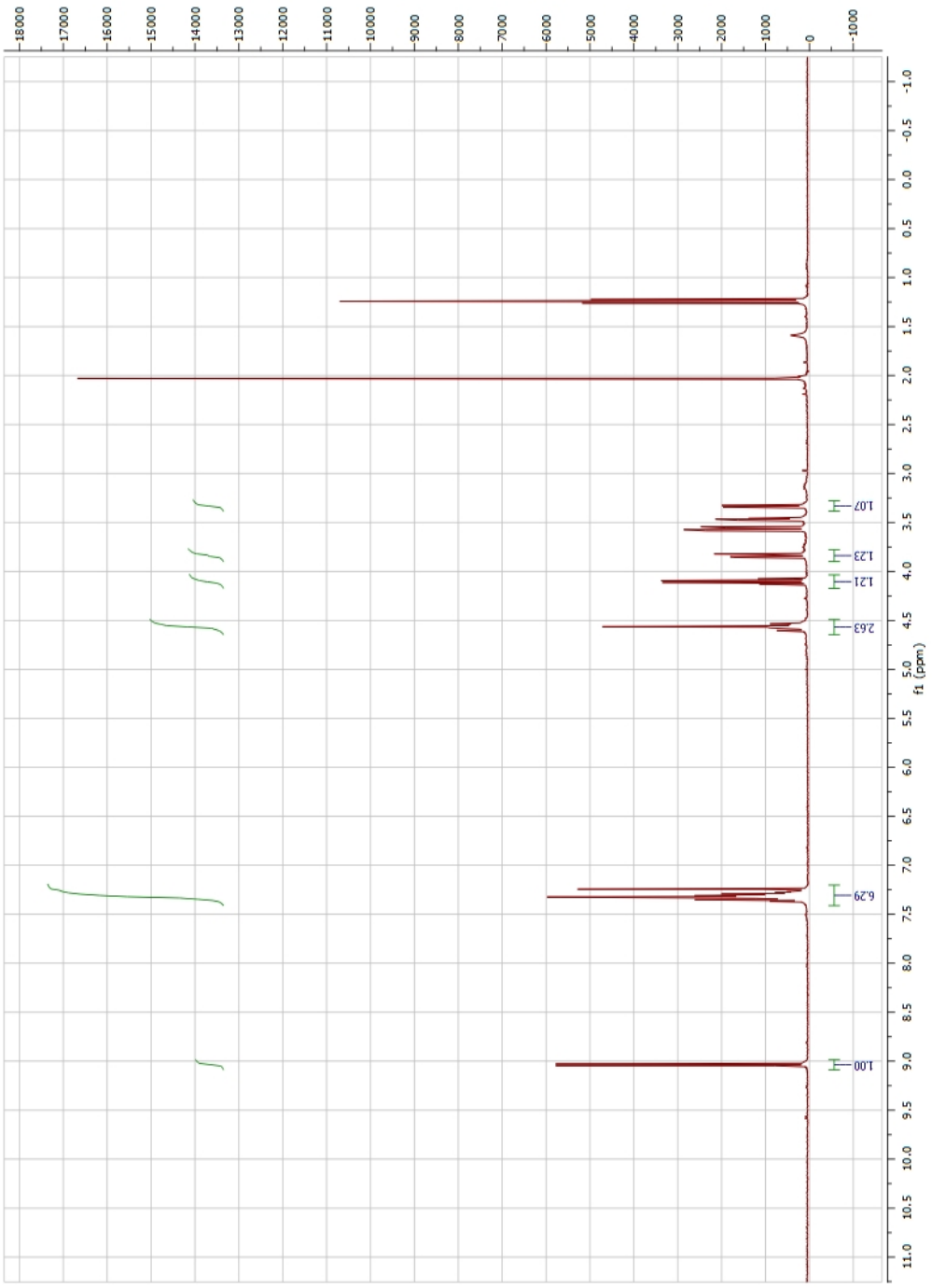

Figure 3.7: H^1 at 400Hz for 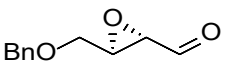

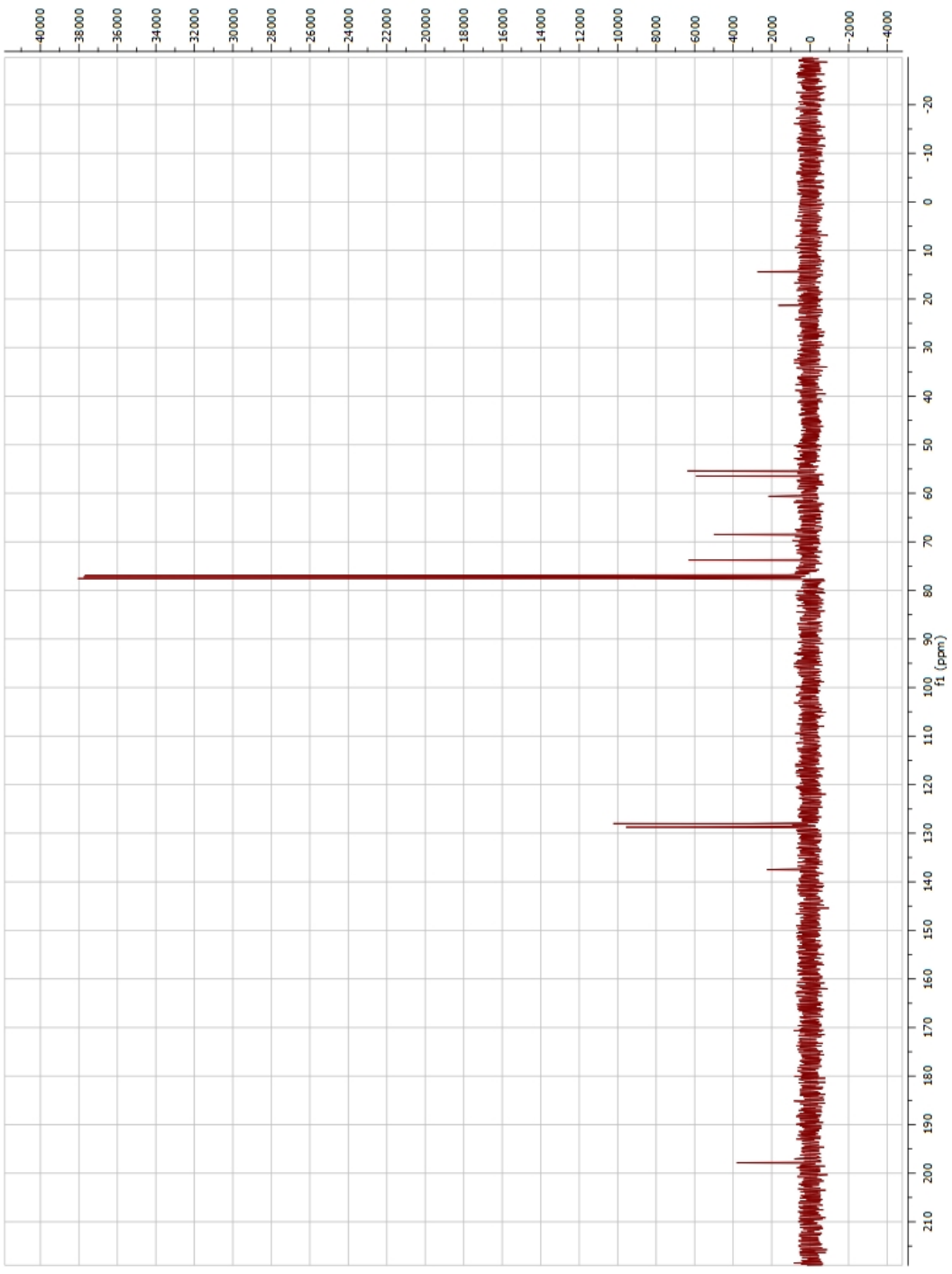

Figure 3.8: C^{13} at 400Hz for 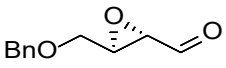

References:

1. Tatibouet, A., et al., *Synthesis and evaluation of fructose analogs as inhibitors of the D-fructose transporter GLUT5.* Bioorgan. Med. Chem., 2000. **8**(7): p. 1825-1833.
2. Yang, J., et al., *Fructose analogs with enhanced affinity for GLUT5.* Diabetes, 2001. **50**: p. A277-A277.
3. Genisson, Y., et al., *Enantioselective access to a versatile 4-oxazolidinonecarbaldehyde and application to the synthesis of a cytotoxic jaspine B truncated analog.* Tetrahedron-Asymmetr., 2007. **18**(7): p. 857-864.
4. Sabitha, G., et al., *Stereoselective total synthesis of (+)-anamarine via cross-metathesis protocol.* Tet. Lett., 2010. **51**(43): p. 5736-5739.
5. Reddy, G.V., et al., *Formal Total Synthesis of (-)-5,6-Dihydrocineromycine B.* Synlett, 2012(18): p. 2677-2681.
6. Maram, L. and B. Das, *A Stereoselective Total Synthesis of Xyolide, a Natural Bioactive Nonenolide.* Helv. Chim. Acta, 2015. **98**(5): p. 674-682.

Chapter 4

Future Work

Although current probes have given insight into transporter-substrate tolerance, gaps remain. ManCou probe's C4 position has the ability for many more functional groups to be added to give further insight into importance of the electron density of the aromatic system as well as how bulky hydrophobic/hydrophilic substitutions may affect uptake. Coumarin functionalization can also affect the color of emission and, if used to target different GLUTs, may allows for simultaneously tracking of the activity of different GLUTs.

4.1 Finish Synthesis of Furanose/Pyranose Probes

With the completion of the ManCou1,2 and 3, strides have been made in understanding substrate and payload tolerance. However how exactly GLUT2 or GLUT5 differentiate between sugar substrates, if they do at all, remains unclear. In Chapter 2 initial work has been done in an attempt to construct a multitude of probes in an attempt to determine this mechanism. Once probe synthesis is completed using a multitude of cellular lines shown to express GLUT5, GLUT2 and neither will need to be exposed to the probes. From their fluorescent uptake or lack thereof, should help determine the substrates specific toward each transporter.

4.2 Develop more ManCou Probes

Current ManCou probes have given interesting insight on transport and transporter/substrate tolerance. However there is significant room for expansion. There are several other amino or hydroxyl coumarins commercially available with differing functional groups that can give insight in hydrophobic tolerance, sterics, sugar-fluorophore linker role,

etc. Manipulating the C4 functional group can also influence the color of the probe as well from violet all the way to red. These probes can shed even more light on the confusing topic of substrate tolerance.

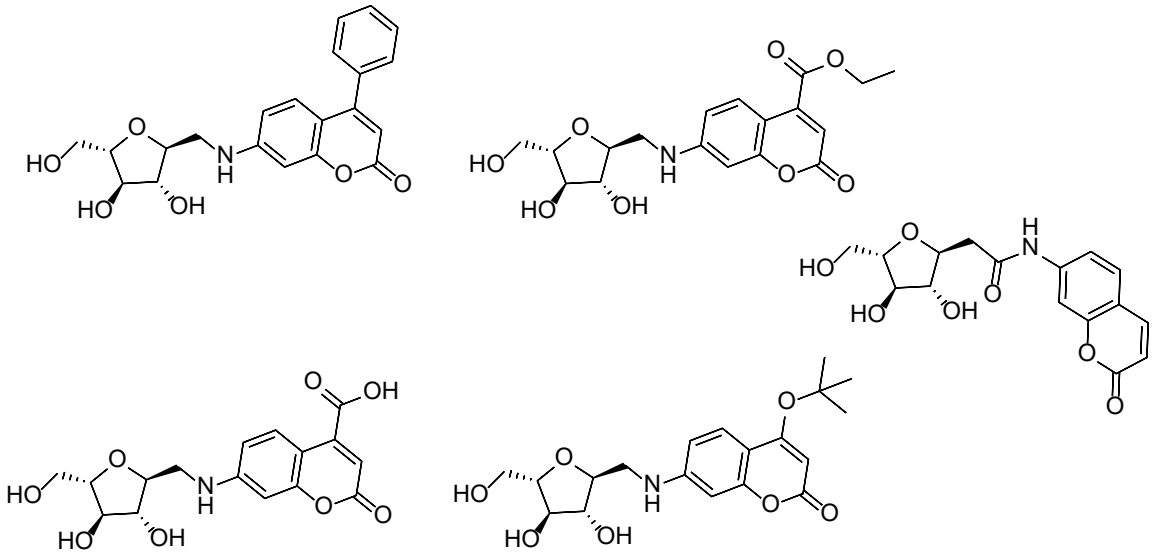

Figure 4.1: Potential future probes

4.3 Multicolor Assay to Measure GLUT Activity

With the construction of ManCou probes and the already tested NBD probes, it is now possible to develop a multicolor assay to measure various GLUT activity simultaneously. Using multiple colors, it will be possible to track the activity of various transporters in real time and potentially diagnose cancer types very quickly and being able to avoid long gene sequencing experiments.